

Lawrence Berkeley National Laboratory

LBL Publications

Title

Nonlinear CO₂ flux response to 7 years of experimentally induced permafrost thaw.

Permalink

<https://escholarship.org/uc/item/7521h0gw>

Journal

Global change biology, 23(9)

ISSN

1354-1013

Authors

Mauritz, Marguerite
Bracho, Rosvel
Celis, Gerardo
[et al.](#)

Publication Date


2017-09-01

DOI

10.1111/gcb.13661

Peer reviewed

Nonlinear CO₂ flux response to 7 years of experimentally induced permafrost thaw

Marguerite Mauritz¹  | Rosvel Bracho² | Gerardo Celis¹ | Jack Hutchings³ | Susan M. Natali⁴ | Elaine Pegoraro¹ | Verity G. Salmon⁵ | Christina Schädel¹ | Elizabeth E. Webb⁶ | Edward A. G. Schuur¹

¹Center for Ecosystem Science and Society, Northern Arizona University, Flagstaff, AZ, USA

²School of Forest Resources and Conservation, University of Florida, Gainesville, FL, USA

³Department of Geological Sciences, University of Florida, Gainesville, FL, USA

⁴Woods Hole Research Center, Falmouth, MA, USA

⁵Environmental Sciences Division and Climate Change Sciences Institute, Oak Ridge National Laboratory, Oak Ridge, TN, USA

⁶Department of Biology, University of Florida, Gainesville, FL, USA

Correspondence

Marguerite Mauritz, Center for Ecosystem Science and Society, Northern Arizona University, Flagstaff, AZ, USA.
Email: marguerite.mauritz@nau.edu

Funding information

Biological and Environmental Research, Grant/Award Number: DE-SC0006982, DE-SC0014085; National Science Foundation, Grant/Award Number: Bonanza Creek LTER program Award # 1026415, CAREER Program Award # 0747195; National Parks Inventory and Monitoring Program

Abstract

Rapid Arctic warming is expected to increase global greenhouse gas concentrations as permafrost thaw exposes immense stores of frozen carbon (C) to microbial decomposition. Permafrost thaw also stimulates plant growth, which could offset C loss. Using data from 7 years of experimental Air and Soil warming in moist acidic tundra, we show that Soil warming had a much stronger effect on CO₂ flux than Air warming. Soil warming caused rapid permafrost thaw and increased ecosystem respiration (R_{eco}), gross primary productivity (GPP), and net summer CO₂ storage (NEE). Over 7 years R_{eco} , GPP, and NEE also increased in Control (i.e., ambient plots), but this change could be explained by slow thaw in Control areas. In the initial stages of thaw, R_{eco} , GPP, and NEE increased linearly with thaw across all treatments, despite different rates of thaw. As thaw in Soil warming continued to increase linearly, ground surface subsidence created saturated microsites and suppressed R_{eco} , GPP, and NEE. However R_{eco} and GPP remained high in areas with large *Eriophorum vaginatum* biomass. In general NEE increased with thaw, but was more strongly correlated with plant biomass than thaw, indicating that higher R_{eco} in deeply thawed areas during summer months was balanced by GPP. Summer CO₂ flux across treatments fit a single quadratic relationship that captured the functional response of CO₂ flux to thaw, water table depth, and plant biomass. These results demonstrate the importance of indirect thaw effects on CO₂ flux: plant growth and water table dynamics. Nonsummer R_{eco} models estimated that the area was an annual CO₂ source during all years of observation. Nonsummer CO₂ loss in warmer, more deeply thawed soils exceeded the increases in summer GPP, and thawed tundra was a net annual CO₂ source.

KEYWORDS

Arctic, carbon, ecosystem respiration, experimental warming, gross primary productivity, net ecosystem exchange, permafrost, thaw, tundra

1 | INTRODUCTION

Permafrost carbon (C) is an important global C sink, representing approximately half of the global soil C stocks (Hugelius et al., 2014;

Köchy, Hiederer, & Freibauer, 2015; Tarnocai, Canadell, Mazhitova, Schuur, & Kuhry, 2009; Zimov, Schuur, & Chapin, 2006). For thousands of years organic C has accumulated in Arctic permafrost soils because cold conditions limited C loss via microbial decomposition

(Ping, Jastrow, Jorgenson, Michaelson, & Shur, 2015; Schuur et al., 2008). In recent decades rapid Arctic warming (Overland et al., 2016; Serreze et al., 2000) has raised permafrost temperatures (Romanovsky et al., 2013) making deep permafrost C vulnerable to microbial decomposition (Dorrepaal et al., 2009; Hicks Pries, Schuur, Natali, & Crummer, 2016; Nowinski, Taneva, Trumbore, & Welker, 2010; Schuur et al., 2008). Decomposition of permafrost C is expected to release CO₂ and CH₄ to the atmosphere and amplify the effects of anthropogenic climate change (Schuur et al., 2015). Many ecosystem models predict greater C uptake across the Arctic (Koven et al., 2011; McGuire et al., 2012) as plants respond positively to warmer air temperatures (Elmendorf et al., 2015; Sturm, Racine, & Tape, 2001; Walker et al., 2006) and offset C loss (Hobbie & Chapin, 1998; Johnson et al., 2000; Oberbauer et al., 2007; Welker, Fahnestock, Henry, O'Dea, & Chimner, 2004). However, these model predictions contradict observed landscape trends toward greater Arctic CO₂ loss (Belshe, Schuur, & Bolker, 2013). Our current knowledge has been largely informed by experiments and models that simulate warmer air temperatures without taking into account the continued exposure of organic soil C as permafrost thaws, therefore underestimating the impact of warming on CO₂ balance (Aerts, Cornelissen, & Dorrepaal, 2006; Koven et al., 2011). Permafrost thaw releases nitrogen (N) (Keuper et al., 2012) and could enhance growth of N-limited plants even more than warmer air temperatures (Chapin, 1983; DeMarco, Mack, Bret-Harte, Burton, & Shaver, 2014; Hobbie & Chapin, 1998; Hobbie, Nadelhoffer, & Hogberg, 2002; Shaver et al., 1998). On the other hand, the permafrost soil C pool far exceeds the vegetation C pool, and greater substrate availability in addition to alleviating N limitation of the microbial community is likely to accelerate decomposition rates and C loss (Abbott et al., 2016; Mack, Schuur, Bret-Harte, Shaver, & Chapin, 2004; Nadelhoffer, Giblin, Shaver, & Laundre, 1991; Weintraub & Schimel, 2003). Future predictions of Arctic C balance thus depend critically on our understanding of how rapidly, and via which mechanisms, permafrost thaw affects C balance (Harden et al., 2012; Koven, Lawrence, & Riley, 2015; McGuire et al., 2016).

Permafrost thaw is coupled to complex soil moisture dynamics because permafrost forms an impermeable layer that prevents water drainage. As permafrost thaws the loss of soil ice structures causes the soil surface to slump and creates saturated soil surface conditions (Jorgenson, Racine, Walters, & Osterkamp, 2001; O'Donnell et al., 2012; Osterkamp et al., 2009). As permafrost recedes deep into the soil (Avis, Weaver, & Meissner, 2011) or drainage channels change (Liljedahl et al., 2016), permafrost thaw can also cause rapid drying. Ecosystem CO₂ losses are expected to be highest in dry, aerobic conditions which stimulate decomposition (Oechel, Vourlitis, Hastings, Ault, & Bryant, 1998; Oechel et al., 1993; Schädel et al., 2016) and limit plant productivity (Chivers, Turetsky, Waddington, Harden, & McGuire, 2009), while anaerobic conditions in saturated sites can limit microbial decomposition and protect permafrost C, even after thaw (Elberling et al., 2013; Sulman et al., 2012). The trajectory of permafrost C loss thus depends on these complex soil moisture dynamics.

The effect of Arctic warming and permafrost thaw is likely to vary across a season due to differences in plant and microbial physiology. Factors that stimulate plant growth early in the spring (Aurela, Laurila, & Tuovinen, 2004; Bosio, Stiegler, Johansson, Mbufong, & Christensen, 2014; Euskirchen, Bret-Harte, Scott, Edgar, & Shaver, 2012; Leffler & Welker, 2013) could stimulate greater summer C storage, while continued microbial decomposition throughout the winter results in C loss that often exceeds summer C storage, even under current climate conditions (Belshe et al., 2013; Euskirchen et al., 2012; Fahnestock, Jones, & Welker, 1999; Oechel, Laskowski, Burba, Gioli, & Kalhori, 2014). Deep thaw and warmer soil temperatures that persist into the winter are expected to increase annual ecosystem C loss as microbial decomposition continues (Larsen, Grogan, Jonasson, & Michelsen, 2007; Trucco et al., 2012; Webb et al., 2016), but photosynthesis is limited by light availability (Euskirchen et al., 2012; Ueyama, Iwata, & Hara-zono, 2014). Evaluating the effect of permafrost thaw on R_{eco} and GPP in different parts of the summer season will provide greater insight to how the ecosystem responds to warming.

The Carbon in Permafrost Experimental Heating Research (CIPEHR) is a warming manipulation that was established in 2008 to directly address the effect of permafrost thaw on C balance of a subarctic tundra ecosystem (Natali et al., 2011). Open top chambers (OTCs) simulate warmer air temperatures similar to other Arctic temperature manipulations (Marion et al., 1997; Oberbauer et al., 2007), while Soil warming is implemented using snow fences paired with spring snow removal that prevents delayed phenology and increased water inputs (Johansson et al., 2013; Walker et al., 1999).

This study used 7 years of summer CO₂ flux data to examine whether the initial increases in R_{eco} and GPP observed after 3 years of warming (Natali, Schuur, Webb, Pries, & Crummer, 2014) could be maintained in the longer term, and what effect continued warming would have on net ecosystem CO₂ exchange (NEE). To gain a more functional understanding of how permafrost thaw impacts CO₂ fluxes we examined thaw, water table depth, air temperatures, and plant biomass as driving variables. We evaluated the effect of warming on R_{eco}, GPP, and NEE early and late in the summer. Winter (nonsummer) R_{eco} estimates, using measurements and site-specific models (Webb et al., 2016), provided context for the annual CO₂ balance of tundra systems undergoing thaw. Overall, our analysis aims to characterize environmental drivers and the seasonal trends in ecosystem CO₂ flux from this thawing tundra ecosystem.

2 | MATERIALS AND METHODS

2.1 | Site description

The Carbon in Permafrost Experimental Heating Research (CIPEHR) experiment is located on a moist acidic tundra site located in the Eight Mile Lake Watershed (−149.23°W, 63.88°N, 670 m). The region is in the discontinuous permafrost zone, but the site itself is underlain entirely by permafrost (Osterkamp et al., 2009). The site is on a gentle, northeast-facing slope with relatively well-drained surface soils. Soil organic C content at the site is 72 kg/m² to 1 m

depth (Plaza et al., submitted), and a 0.25-m–0.35-m-thick organic horizon overlies cryoturbated glacial till and loess mineral soils. Mean annual temperatures in the area averaged -0.94°C from 1977 to 2015 (SE: 0.25°C ; summer mean: 11.91°C (SE: 0.22°C); nonsummer mean: -10.09°C (SE: 0.33°C)) and -1.68°C from 2009 to 2015 (SE: 0.82°C ; Healy and McKinley Stations, Western Regional Climate Center and NOAA National Centers for Environmental Information). Permafrost in the watershed has been warming since 1985 (Osterkamp et al., 2009), and maximum seasonal extent of permafrost thaw (active layer thickness) was approximately 50 cm when the experiment was installed in 2008 (Natali et al., 2011). Vegetation at CiPEHR is typical of moist acidic tundra, dominated by the tussock forming sedge *E. vaginatum*. More detailed descriptions of vegetation can be found elsewhere (Deane-Coe et al., 2015; Natali, Schuur, & Rubin, 2012; Salmon et al., 2016).

2.2 | Experimental design

CiPEHR was designed to simulate the effect of warmer air and soil temperatures and permafrost degradation on ecosystem C exchange. Soil warming was initiated in the winter of 2008/2009, and Air warming in April 2009. Air warming was achieved using polycarbonate open top chambers (cubicle OTCs: $0.36\text{ m}^2 \times 0.5\text{ m}$ tall). Soil warming was achieved passively, using snow fences ($1.5\text{ m} \times 8\text{ m}$), which accumulated snow on the leeward side and insulated the ecosystem in the winter. The treatments were applied in a blocked split-plot design, with three blocks located in similar areas of the landscape within 100 m of each other. Each block contained two replicate snow fences ($n = 6$ snow fences), and nested within each snow fence were eight plots ($0.6\text{ m} \times 0.6\text{ m}$); Air warming treatments were applied to two plots on each side of the fence. There were a total of 48 plots with four treatment combinations: Control, Air warming, Soil warming, Air & Soil warming. On the windward side of the fences snow depth varied with ambient winter precipitation (Table 1). To avoid artifacts such as increased water input and delayed phenology (Walker et al., 1999), the increased snowpack was manually removed in the spring to match the ambient snowpack. Full details can be found in Natali et al. (2011, 2014), but note the change in treatment names: Air warming was formerly called summer warming, Soil warming was winter warming, and Air & Soil warming was annual warming.

2.3 | Environmental variables

Meteorological conditions were monitored half-hourly using a HOBO Onset station (Bourne, MA, USA). The station measured air temperature ($^{\circ}\text{C}$) at 2 m and photosynthetically active radiation (PAR, $\mu\text{mol m}^2\text{ s}^{-1}$) year-round; rainfall (mm) was measured during the summer season only. Missing meteorological data were gap-filled from NOAA stations in the area (Western Regional Climate Center). Chamber air temperatures were measured every 1.5 hrs within each individual OTC at 15 cm height using shaded thermistors. Soil temperatures were measured half-hourly at 5 and 10 cm depth in every

plot and at 20 and 40 cm in half the plots of each treatment using type T copper-constantan thermocouples. Water table depth (WTD) was measured throughout the summer season as in Vogel, Schuur, Trucco, and Lee (2009) at two wells on both sides of the fence, three times a week from 2009 to 2012, and at three wells per fence side twice a week from 2013 to 2015. Although WTD was not measured at each plot, WTD was assigned to each plot based on proximity to WTD wells. Active layer thickness (ALT) was measured adjacent to every plot during the same week in mid-September (week 36) of each year. Annual measurements inside plots showed that Air warming did not significantly impact thaw depths (paired *t*-test, $p > .05$).

2.4 | Carbon dioxide flux measurements

Chambers were deployed from 1 May to mid-September, determined by spring snowmelt and autumn snowstorms. Net ecosystem CO_2 exchange (NEE) was monitored during the summer season using an automated chamber system. To maintain the Air warming treatment, CO_2 flux chambers on the Air and Air & Soil warming had dimensions identical to OTCs ($0.36\text{ m}^2 \times 0.5\text{ m}$). Chambers measuring Control and Soil warming were half the height ($0.36\text{ m}^2 \times 0.25\text{ m}$) and fans circulated air continuously to prevent warmer air inside the chambers. Chambers were connected to a closed path infrared gas analyzer (LI-820; LICOR Corp., Lincoln, NE, USA) and sampled using a data logger (CR1000; Campbell Scientific). Each chamber was sampled every 1.6 hr. During a flux measurement, CO_2 concentration and air temperature were measured for 1.5 mins and logged every 2 s, while fans circulated air. Flux rates were determined using linear regression and converted from volumetric ($\text{ppm CO}_2\text{ m}^2\text{ s}^{-1}$) to mass ($\mu\text{mol CO}_2\text{ m}^{-2}\text{ s}^{-1}$) using plot-specific chamber volumes and air temperatures. A recent analysis showed CO_2 fluxes and light response curves from Control plots were comparable to ambient tundra fluxes monitored at an adjacent eddy covariance tower (Celis et al., in review) indicating that there was no adverse effect of chambers on CO_2 fluxes (but see statistical analysis for a note on 2009). Details on filtering can be found in the supplement.

2.5 | Flux partitioning and cumulative estimates

The summer season was defined from May 1 to September 30 for gap-filling purposes and cumulative summer estimates. Fluxes were gap-filled to create half-hourly net ecosystem exchange (NEE) and ecosystem respiration (R_{eco}) fluxes. Ecosystem respiration was modeled with soil temperature at 10 cm using an exponential Arrhenius-type equation (Natali et al., 2011, 2014). Parameters were estimated for each plot under low light conditions ($\text{PAR} < 5\ \mu\text{mol m}^2\text{ s}^{-1}$), using data from the entire summer season. The temperature relationship was used to gap-fill missing data and estimate R_{eco} when $\text{PAR} < 5\ \mu\text{mol m}^2\text{ s}^{-1}$. At $\text{PAR} > 5\ \mu\text{mol m}^2\text{ s}^{-1}$, NEE was gap-filled using a hyperbolic light response curve. The NEE model was parameterized for each plot on a monthly basis using site-level PAR, adjusted for light reduction through the chambers. Measured PAR

TABLE 1 Environmental variables measured at the site or treatment level during the summer (May–September) or non-summer (October–April)

Variable	Treatment	Season	Year						
			2009	2010	2011	2012	2013	2014	2015
Air temperature (°C)	Site level	Summer	9.71	9.84	9.42	9.17	9.27	9.13	9.53
		Non-summer	-12.78	-9.20	-11.10	-12.30	-13.74	-8.15	-8.13
		Annual	-3.35	-1.24	-2.50	-3.30	-4.00	-0.90	-0.71
Cumulative precipitation (mm)	Site level	Summer	178	250	164	223	138	570	354
PAR (mean) ($\mu\text{mol m}^{-2} \text{s}^{-1}$)	Site level	Summer	376.59	362.42	378.70	366.67	412.78	344.45	358.01
		Non-summer	141.86	66.11	114.43	123.45	125.66	120.31	112.52
Snow depth (April) (m)	Control (no Soil warming)		0.50 (0.09)	0.23 (0.01)	0.27 (0.04)	0.59 (0.02)	0.75 (0.03)	0.23 (0.01)	0
	Soil warm		0.92 (0.04)	0.44 (0.01)	0.75 (0.01)	1.13 (0.03)	1.01 (0.02)	0.60 (0.01)	0.45 (0.02)
Date snow free (DOY)	Control (no Soil warming)		No data	117 (1)	117 (2)	125 (1)	147 (1)	111 (2)	112 (2)
	Soil warm		No data	117 (1)	117 (2)	125 (1)	147 (1)	111 (2)	112 (2)
Chamber air temperature (°C)	Control	Summer	12.45 (0.50)	11.55 (0.27)	10.48 (0.48)	11.19 (0.11)	13.19 (0.33)	10.17 (0.34)	11.15 (0.14)
	Air		12.70 (0.45)	11.86 (0.24)	11.05 (0.43)	11.49 (0.11)	13.60 (0.59)	10.85 (0.38)	11.38 (0.25)
	Soil warm		12.40 (0.51)	11.54 (0.16)	10.67 (0.46)	10.99 (0.17)	13.35 (0.56)	10.48 (0.35)	11.32 (0.47)
	Air & Soil		12.69 (0.63)	11.94 (0.17)	11.10 (0.42)	11.65 (0.10)	13.82 (0.58)	10.85 (0.36)	11.35 (0.19)
Active layer thickness (cm)	Control	Summer	53.06 (0.98)	56.93 (0.96)	55.20 (0.77)	60.89 (0.71)	64.15 (1.64)	63.42 (1.15)	63.96 (1.84)
	Air		52.39 (1.41)	57.10 (0.90)	54.28 (1.24)	59.18 (0.67)	62.81 (1.49)	65.17 (2.09)	62.10 (1.90)
	Soil warm		55.86 (0.67)	63.56 (2.03)	62.62 (2.34)	70.28 (2.59)	77.25 (2.59)	84.96 (3.85)	91.44 (2.42)
	Air & Soil		52.96 (0.88)	61.71 (0.75)	59.00 (1.50)	67.58 (1.97)	72.78 (2.71)	80.63 (3.79)	90.83 (4.08)
Surface soil temperature (°C) (5 and 10 cm)	Control	Summer	5.48 (0.53)	6.09 (0.46)	5.38 (0.32)	6.42 (0.40)	6.36 (0.33)	5.48 (0.36)	5.32 (0.31)
	Air		5.46 (0.31)	6.31 (0.39)	5.26 (0.31)	6.25 (0.37)	6.09 (0.28)	4.8 (0.35)	4.76 (0.37)
	Soil warm		5.90 (0.20)	6.14 (0.35)	5.60 (0.33)	6.46 (0.24)	6.27 (0.32)	5.15 (0.38)	4.96 (0.40)
	Air & Soil		5.74 (0.28)	5.90 (0.28)	5.54 (0.31)	6.33 (0.23)	6.14 (0.24)	5.22 (0.28)	4.82 (0.29)
	Control	Non-summer	-3.30 (0.49)	-4.84 (0.25)	-4.49 (0.23)	-3.30 (0.39)	-1.94 (0.27)	-1.73 (0.15)	-2.31 (0.17)
	Air		-3.16 (0.23)	-5.07 (0.28)	-4.56 (0.23)	-3.31 (0.28)	-1.88 (0.22)	-1.55 (0.23)	-2.09 (0.17)
	Soil warm		-1.88 (0.24)	-3.26 (0.22)	-2.17 (0.26)	-1.55 (0.15)	-1.31 (0.18)	-0.64 (0.11)	-0.64 (0.09)
	Air & Soil		-2.08 (0.24)	-3.57 (0.33)	-1.97 (0.22)	-1.60 (0.25)	-1.48 (0.27)	-0.76 (0.20)	-0.61 (0.13)

(Continues)

TABLE 1 (Continued)

Variable	Treatment	Season	Year						
			2009	2010	2011	2012	2013	2014	2015
Deep soil temperature (°C) (20 and 40 cm)	Control	Summer	1.19 (0.20)	1.49 (0.23)	1.15 (0.16)	1.69 (0.21)	1.57 (0.21)	1.44 (0.17)	1.25 (0.13)
	Air warm		1.04 (0.13)	1.63 (0.12)	1.12 (0.13)	1.68 (0.15)	1.46 (0.19)	2.42 (0.24)	1.87 (0.16)
	Soil warm		1.25 (0.08)	2.18 (0.21)	1.86 (0.16)	2.76 (0.17)	2.37 (0.22)	1.42 (0.19)	1.23 (0.14)
	Air & Soil warm		1.12 (0.13)	1.93 (0.24)	1.74 (0.24)	2.69 (0.27)	2.33 (0.28)	2.47 (0.27)	2.34 (0.24)
	Control	Non-summer	-1.81 (0.18)	-3.25 (0.09)	-3.01 (0.15)	-1.77 (0.23)	-0.96 (0.14)	-0.73 (0.05)	-1.19 (0.09)
	Air warm		-1.20 (0.11)	-3.28 (0.06)	-3.01 (0.13)	-1.54 (0.13)	-0.86 (0.16)	-0.23 (0.02)	-0.25 (0.02)
	Soil warm		-0.72 (0.12)	-2.31 (0.24)	-1.06 (0.13)	-0.61 (0.06)	-0.53 (0.05)	-0.87 (0.06)	-1.44 (0.11)
	Air & Soil warm		-0.79 (0.08)	-2.34 (0.21)	-1.11 (0.08)	-0.52 (0.03)	-0.51 (0.04)	-0.28 (0.04)	-0.28 (0.04)
Number of weeks frozen (weekly mean at 40 cm < -2°C)	Control		11	16	15	10	0	4	6
	Air warm		12	16	14	7	1	0	3
	Soil warm		2	14	5	0	0	0	0
	Air & Soil warm		3	14	5	0	0	0	0
Water table depth (cm)	Control (no soil warming)	Summer	-27.64 (0.69)	-20.30 (0.33)	-23.78 (0.27)	-22.13 (0.32)	-23.82 (0.44)	-14.49 (0.63)	-14.94 (0.68)
	Soil warm		-25.42 (0.73)	-17.47 (1.17)	-20.43 (0.77)	-16.52 (1.50)	-21.79 (0.84)	-9.10 (0.68)	-8.33 (1.07)

In 2013 mean chamber temperatures were almost 2°C higher than in other years, because Air warming only occurred during the snow-free period between June and September; May–September temperatures in 2013, based on chamber-specific regressions with site air temperature, were Control: 10.18°C, Air: 9.9°C, Soil: 10.10°C, Air & Soil: 10.3°C. If no Air warming treatment is listed, then measurements occurred at the fence level and Control (no Soil warming) includes both Control and Air warming treatments, while Soil warm includes both Soil and Air & Soil warming treatments. Bold letters indicate a significant effect of the treatment across all years, except WTD, which was tested for year-specific treatment effects to capture trends through time. See Tables S1 and S2 for variable-specific coefficients. Values in parentheses are standard error.

was used for gap filling. Gross primary productivity was estimated when $PAR \geq 5 \mu\text{mol m}^{-2} \text{s}^{-1}$, such that $GPP = NEE + R_{\text{eco}}$. We use the convention that positive NEE values represent a net ecosystem CO_2 sink, and negative NEE values represent a net CO_2 source.

In May 2009 individual plot locations were not yet finalized so fluxes were estimated at the treatment level for each fence. In May 2013 CO_2 flux chambers could not be deployed because there was still snow on the ground. Therefore in May 2013, NEE, R_{eco} , and GPP were estimated at each plot, for the whole month, using a non-summer model for R_{eco} and nearby eddy tower measurements to constrain GPP (Webb et al., 2016). Details on gap filling can be found in the supplement.

Cumulative fluxes were calculated from half-hourly flux rates and reported in $\text{g CO}_2\text{-C m}^{-2}$. Early and late season fluxes were determined based on the week of transition between average source and sink (Table 2 and Appendix S1). Annual CO_2 fluxes were estimated using site-specific nonsummer R_{eco} models from Webb et al. (2016). Upper and lower constraints on annual CO_2 losses were determined with models that represent our best estimate of nonsummer R_{eco} loss (snow pit), and the highest R_{eco} loss (eddy).

2.6 | Aboveground biomass measurements

Live aboveground vascular plant and moss biomass were measured at peak summer season (July) from 2009 to 2013 using the point-intercept method (Salmon et al., 2016; Schuur, Crummer, Vogel, & Mack, 2007). In 2011 and 2013–2015 plot-level NDVI photographs (Tetracam ADC) were taken weekly. The relationship between peak NDVI and total biomass was used to predict total biomass (Boelman et al., 2003) in 2014 and 2015 (Fig. S1a, total biomass = $1770 \cdot \text{NDVI} - 839$; $r^2 = .33$). Treatment differences were smaller when total biomass was estimated from NDVI compared to point-intercept method; however, the overall treatment and temporal patterns in 2011 and 2013 were similar with both methods (Fig. S1b,c).

2.7 | Statistical analysis

All analyses were conducted in R (R Core Team 2015). Mixed effects models (lme4, Bates, Mächler, Bolker, & Walker, 2015) were used to

investigate effects of treatments, changes over time, and relationships between fluxes, environmental variables, and biomass. Normality of variables was determined with visual inspection of data and model residuals, and data were log-transformed when necessary. All analyses included a random effect to account for repeated measures and spatial nesting inherent in the experimental design (Barr, Levy, Scheepers, & Tily, 2013), with plot nested in Soil warming, nested in fence, nested in block. Random year effects were included to account for year-to-year variation or as a continuous fixed effect and random slope variable when explicitly testing changes through time (see Appendix S1 for details). Treatment effects were visualized as the difference between Control and treatment; differences were calculated between Control (mean of two plots) and treatment (mean of two plots) at every fence ($n = 6$, per treatment).

To gain a functional understanding of the CO_2 flux response to thaw, we tested the effect of ALT, WTD, chamber air temperature, and plant biomass. Correlation between predictors was tested using a variable inflation factor (VIF) test, and variables were standardized to compare effect sizes. Active layer thickness was included as a random slope effect, and all interactions were allowed because we expected complex interactions. Backward step-wise model selection was used to eliminate variables that resulted in less than 5 AIC change (Pinheiro & Bates, 2000; Zuur, Ieno, Walker, Saveliev, & Smith, 2009). Residuals from multiple variable models were analyzed for treatment effects to evaluate whether any remaining variance was explained by treatments (Patrick, Ogle, Bell, Zak, & Tissue, 2009). To determine the shape of the thaw response we fit an ALT model with linear (ALT) and quadratic (ALT + ALT²) fixed effects and random slopes, with and without treatment effects. The best fitting, simplest model was selected based on a 5 AIC improvement.

We report AIC, marginal R^2 (fixed effects), and conditional R^2 (fixed and random effects) from the MUMIN package (Bartón, 2016; Johnson, 2014; Nakagawa & Schielzeth, 2013). Variable significance was determined using bootstrapped 95% confidence intervals (CI). A CI spanning zero was considered nonsignificant, and 95% CI are reported in parentheses in the results, unless otherwise stated.

For all analyses investigating treatment effects over time, Control 2009 was set as the reference level and is represented by the intercept. In these models a significant year effect indicates a change in

TABLE 2 First week of transition from source to sink (NEE <0 or NEE = 0) early in the summer and from sink to source (NEE = 0) late in the summer for each treatment and year

Treatment	Week of source/sink transition													
	2009		2010		2011		2012		2013		2014		2015	
	Early	Late	Early	Late	Early	Late	Early	Late	Early	Late	Early	Late	Early	Late
Control	19	32	22	34	22	36	22	35	22	36	18	35	21	35
Air	21	32	22	34	21	36	22	35	22	35	<18	35	<18	35
Soil	21	32	21	34	22	36	22	35	22	36	21	35	21	32
Air & Soil	21	32	21	33	22	36	22	35	22	36	18	35	<18	35
Week used	22	35	22	35	22	35	22	35	22	35	22	35	22	35

Seasonal fluxes were calculated based on a common time period; early: prior to and including week 22 (beginning June), and late: including and following week 35 (end August).

Control; a significant treatment*year interaction means the treatment effect was different from the treatment effect in 2009. For example, a significant increase in Air warming in 2009 and nonsignificant Air*2010 indicate that the effect of Air warming was no different in 2010 than in 2009, and Air warming significantly increased flux relative to Control in both years (i.e., Figure 2a and Table 3).

In 2009, NEE was surprisingly low compared to chamber and eddy covariance estimates in an adjacent watershed (Belshe, Schuur, Bolker, & Bracho, 2012; Trucco et al., 2012). We suspect root disturbance from installing the experiment suppressed CO₂ fluxes, but were recovered a year later (2010) (Celis et al., in review). The ability of the system to respond to treatments was not impaired (Natali et al., 2011), but to avoid overestimating the changes in CO₂ flux over time, temporal trends in Control are reported relative to 2010

(Table S6). In regression analyses, 2009 was excluded to avoid overestimating the response of CO₂ fluxes to increasing ALT.

Data in this paper are archived at Bonanza Creek LTER Data Catalog: <http://www.lter.uaf.edu/data/data-catalog>.

3 | RESULTS

3.1 | Environmental factors

3.1.1 | Ambient conditions

Summer season (May–September) average air temperatures were similar across years, ranging from 9.13 to 9.84°C. Nonsummer temperatures were more variable, ranging from –13.74 to –8.13°C (Table 1). Precipitation varied between 138 and 354 mm; 2013 had

TABLE 3 The effect of treatments on summer season cumulative Reco, GPP, and NEE in each year of measurement

Variable	Reco			GPP			NEE		
	Change (%)	Min CI	Max CI	Change (%)	Min CI	Max CI	Change (%)	Min CI	Max CI
Intercept (2009)	195.27	173.34	219.53	201.60	174.44	232.97	4.96	–17.24	35.56
Air	19.30	3.80	38.51	20.86	–0.55	47.00	50.66	–605.91	924.05
Soil	7.26	–8.17	25.53	2.28	–16.89	25.82	–204.52	–772.26	578.39
Air*Soil	–5.72	–23.98	16.03	–4.29	–27.44	26.62	–19.87	–741.95	1184.71
2010	35.75	19.83	54.59	41.17	22.68	63.28	213.04	–292.66	809.45
2011	18.84	4.98	34.99	36.54	17.89	58.17	797.16	165.05	1514.12
2012	52.83	35.08	73.38	84.73	60.42	112.73	1348.35	597.63	2264.37
2013	55.64	37.05	76.62	94.90	69.51	123.67	1651.60	846.52	2639.30
2014	70.06	50.30	92.57	116.89	88.55	149.92	1943.54	1058.64	3014.25
2015	98.77	75.66	126.26	141.90	109.34	179.90	1806.05	976.37	2787.14
Air*2010	–4.95	–20.64	12.41	0.19	–17.75	21.45	190.86	–246.04	858.95
Air*2011	0.12	–16.28	19.56	4.48	–14.64	27.62	153.23	–277.66	818.04
Air*2012	–9.38	–25.03	8.55	–8.29	–25.09	11.82	66.69	–347.90	667.45
Air*2013	–12.10	–26.72	4.99	–10.79	–26.62	8.09	26.13	–388.92	623.02
Air*2014	–21.89	–34.85	–6.98	–19.88	–34.68	–2.14	–37.28	–428.39	536.68
Air*2015	–25.12	–37.57	–11.11	–19.18	–34.08	–1.44	51.09	–344.50	651.33
Soil*2010	14.53	–3.74	35.70	28.11	4.94	55.96	597.39	–113.32	1606.16
Soil*2011	35.99	13.57	61.91	55.53	26.77	90.22	865.10	105.45	1980.43
Soil*2012	37.70	15.31	64.63	47.56	21.38	78.64	704.46	–46.88	1753.37
Soil*2013	42.50	19.36	70.32	48.78	21.66	81.62	616.56	–82.29	1574.32
Soil*2014	17.72	–1.54	40.53	11.96	–8.41	36.88	–107.12	–610.99	592.25
Soil*2015	–9.74	–24.33	7.43	–9.62	–26.15	9.68	–236.21	–693.35	395.77
Air*Soil*2010	–11.32	–30.49	14.50	–18.24	–38.44	8.59	478.87	–733.85	534.29
Air*Soil*2011	–21.26	–38.81	1.36	–28.09	–45.85	–4.56	693.47	–791.00	412.36
Air*Soil*2012	–15.18	–34.48	9.51	–18.95	–39.24	8.34	564.70	–708.90	593.94
Air*Soil*2013	–19.18	–37.35	4.16	–23.21	–41.80	1.92	494.23	–720.77	587.43
Air*Soil*2014	9.99	–14.46	42.15	7.41	–19.92	43.87	85.87	–485.67	1164.28
Air*Soil*2015	31.33	2.63	70.50	31.67	–0.93	75.87	189.35	–221.47	1839.74

All data were log-transformed, so model coefficients are shown as a percent change from their reference category. Control in 2009 was set as the reference and is therefore represented by the intercept, in g CO₂–C m^{–2}. All treatment effects are relative to 2009 (grey highlight). Bold values indicate significant effects. A significant treatment*year interaction means the effect was significantly different from 2009; a non-significant treatment*year interaction means the effect in that year was the same as in 2009.

the lowest precipitation and 2015 the highest (Table 1). In most years the experiment, and surrounding tundra, were snow-free by the end of April, and that was used to guide the timing of CO₂ flux measurements and the start of Air warming manipulations. Ambient snow pack ranged from low, patchy snow cover in 2015 to 0.75 m in 2013. In contrast to all other years, the snow pack in 2013 persisted to late May, almost an entire month longer than was typical (Table 1).

3.1.2 | Experimental conditions

Plots on the leeward side of the snow fence (Soil and Air & Soil warming) experienced the same ambient air temperature and precipitation but accumulated more snow, as designed. Mean elevated snow pack depth measured in April, prior to snow removal, ranged from 0.45 m in the lowest snow accumulation year (2015) to >1 m in high snow years (Table 1). Variation in mean snow pack depth was mainly due to variable snow volume, which depended both on ambient snowfall and on periodic redistribution by wind. Despite large interannual variation in snowfall, treatment plots were always covered, and the maximum height of snow pack on the leeward side of fences was controlled by the height of the fences and was similar across years.

Insulation under the snow pack increased nonsummer surface soil temperatures (5 and 10 cm) by 1.49°C (1.16–1.81°C) and deep soils (20 and 40 cm) by 1.05°C (0.83–1.27°C) across years (Table 1, Table S1, Fig. S2). As a result of Soil warming, ALT in Soil and Air & Soil warming increased at a rate of ~6 cm/year, from 2009 to 2015 (Figure 1a, Table S1). In Control and Air warming ALT increased ~2 cm/year, a slower, but still significant rate of thaw. After the first two winters of snow manipulation, deep Soil warming persisted into the summer (0.78°C average increase, CI: 0.35–1.20°C, Table 1, Table S1, Fig. S2). In contrast, surface soil temperatures (5 and 10 cm) did not differ between treatments during the summer. Air temperatures inside Air and Air & Soil warming chambers were on average 0.4°C (CI: 0.29–0.51°C) warmer throughout the summer than Control and Soil warming (Table 1, Table S1).

Water table depths in Soil and Air & Soil warming were closer to the surface (wetter) compared to Control and Air warming in all years, but the difference was significant only in the highest precipitation years (Soil₂₀₁₂ 0.88–3.38 cm, Soil₂₀₁₄ 1.75–6.76 cm, Soil₂₀₁₅ 4.02–9.09 cm, Figure 1b, Table 1 and Table S2). Higher water table at Soil and Air & Soil warming was likely due to ground surface subsidence rather than greater water inputs because accumulated snow was removed each year. Heterogeneous patterns of ground surface subsidence observed in the Soil and Air & Soil warming resulted in some plots remaining dry (less subsidence), while the water table at other plots was at or above the ground surface (more subsidence), particularly in 2014 and 2015 (Fig. S3) when precipitation was high and subsidence was substantially progressed.

3.2 | Cumulative summer season CO₂ fluxes

Both Soil and Air & Soil warming significantly increased ecosystem C loss via R_{eco}. This effect was initially small but became larger each

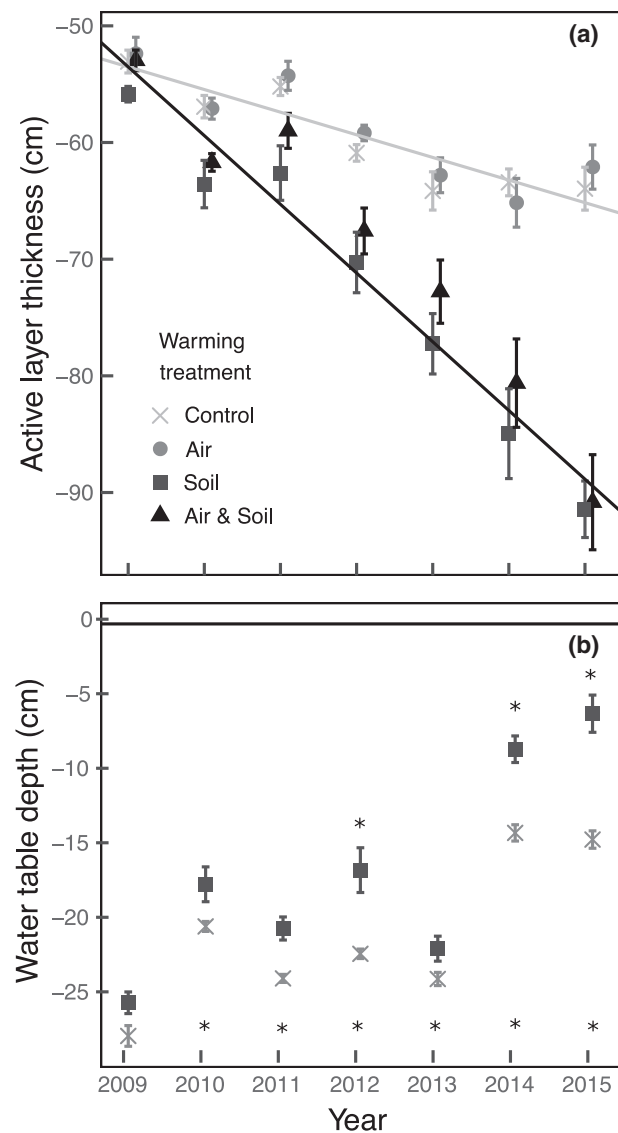


FIGURE 1 Active layer thickness for each treatment and year (a), and summer mean water table depth measured at wells within the footprint of the Control and Soil warmed sides of the fence (b). Water table depths represent the whole footprint of the Control (ambient snow) and Soil warmed (deep snow) sides of the fences and include air-warmed treatments. For water table depth, stars above the square indicate significance of Soil warming in each respective year, and stars along the x-axis indicate a significant change in Control compared to 2009. Symbols are slightly offset to make them easier to distinguish. Error bars are standard error

year, through 2013 (Soil₂₀₁₁ 14%–62%; Soil₂₀₁₂ 15%–65%; Soil₂₀₁₃ 19%–70%; Figure 2a, Table 3). Soil and Air & Soil warming also increased GPP through 2013, with significantly higher GPP 1 year earlier than R_{eco} (Soil₂₀₁₀ 5%–56%; Soil₂₀₁₁ 27%–90%; Soil₂₀₁₂ 21%–79%; Soil₂₀₁₃ 22%–82%; Figure 3b, Table 3). Treatment patterns changed in 2014 and 2015 as the treatment effects on R_{eco} and GPP decreased, particularly in Soil and Air & Soil warming (Figure 2a,b, Table 3).

Air warming caused a slight increase in R_{eco} (Air: 4%–39%; Figure 2a, Table 3) through 2013, with a similar, but nonsignificant,

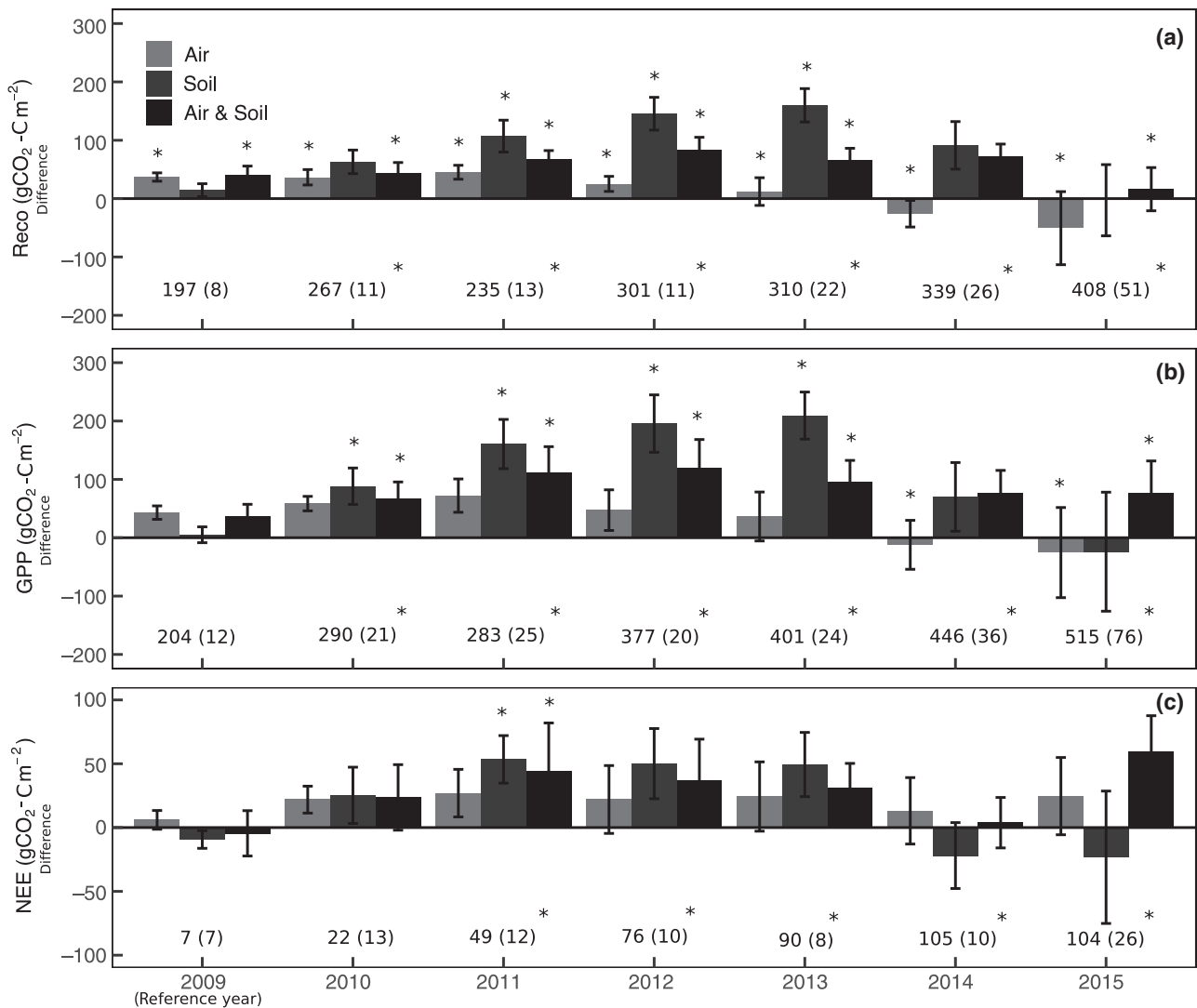


FIGURE 2 Difference in cumulative R_{eco} (a), gross primary productivity (GPP) (b), and net ecosystem CO_2 exchange (NEE) (c) $\text{g CO}_2 \text{ m}^{-2}$ in each year of warming, calculated as treatment—Control. Numbers in the figure are cumulative fluxes for Control treatments. Stars above bars indicate significance of the treatment in each year, and stars next to text indicate a significant change in Control compared to 2009. Error bars are standard errors

pattern for GPP (Figure 2b, Table 3). The effect of Air warming on R_{eco} and GPP declined over time and by 2014 and 2015 was significantly lower relative to Control treatments (R_{eco} : Air₂₀₁₄ -35% to -7% ; Air₂₀₁₅ -38% to -11% ; GPP: Air₂₀₁₄ -35% to -2% ; Air₂₀₁₅ -34% to -1% , Figure 2a,b, Table 3).

After year one, NEE in all treatments trended higher than Control through 2013, but was significantly higher only in 2011 for Soil and Air & Soil warming (Soil₂₀₁₁ 105%–1980%; Figure 2c, Table 3). In 2014 and 2015, NEE in treatments declined relative to Control, especially in Soil warming (Figure 2c).

The changing effects of Air warming and Soil warming through time were due to shifts in the tundra response to treatments, as well as concurrent changes in the Control. Ecosystem respiration in the Control increased by 10%–20% each year, while GPP increased by 20%–40% each year (Table 3). By 2015, mean Control R_{eco} was 45% higher, while GPP increased by 70% since 2010 (Table S3). This resulted in a fivefold increase in NEE from 22 $\text{g CO}_2 \text{ m}^{-2}$

($\pm 13 \text{ g CO}_2 \text{ m}^{-2}$) in 2010 to 104 $\text{g CO}_2 \text{ m}^{-2}$ ($\pm 26 \text{ g CO}_2 \text{ m}^{-2}$) by 2015 (Figure 2c).

3.3 | Aboveground biomass

Patterns of aboveground plant biomass largely showed the same pattern as R_{eco} and GPP measurements. Plant biomass was, on average, 17% higher in Soil and Air & Soil warming treatments compared to Control, across all years (Biomass_{Soil} 2%–35%; Table S4). On a year-by-year basis, the increase in Soil and Air & Soil treatments was statistically significant from 2011 to 2012 (Soil₂₀₁₁ 4%–65%; Soil₂₀₁₂ 2%–61%; Figure 3, Table S5). In 2013, and beyond, the effect of Soil and Air & Soil warming declined and was no longer statistically significant. Air warming had a small positive effect on biomass in some years, but was not significantly different from Control. Biomass in Control increased by 55% from 2009 to 2015 (Biomass₂₀₁₅ 32%–83%; Figure 3, Table S5).

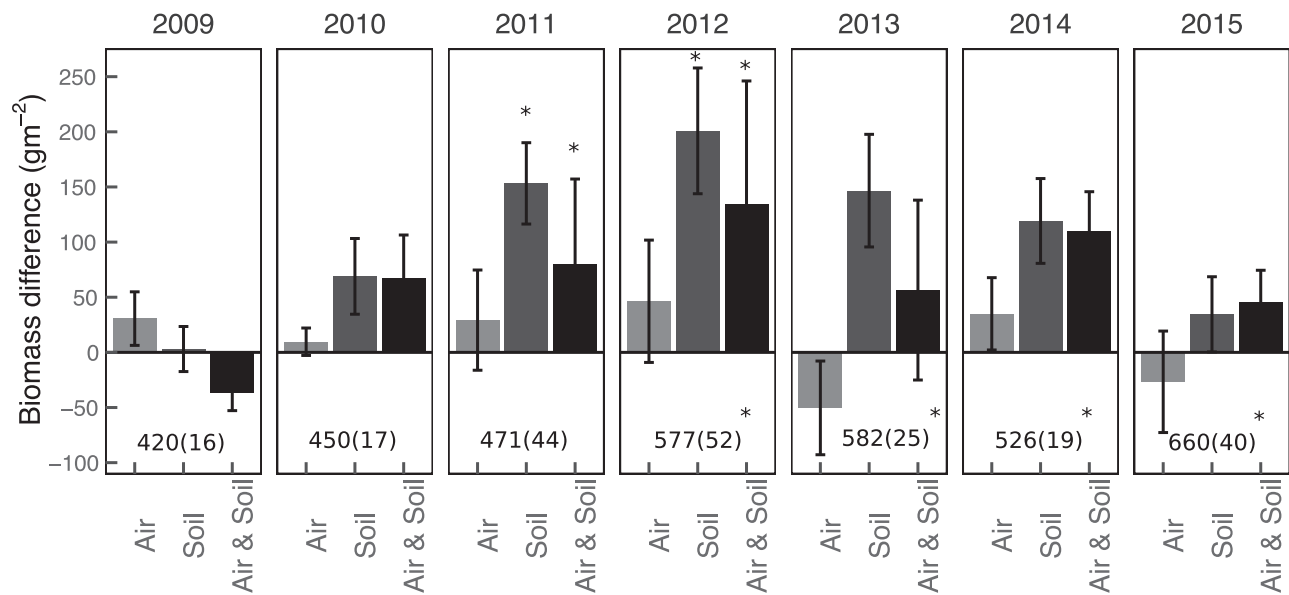


FIGURE 3 Difference in total above ground biomass (g m^{-2}) in each year of warming, calculated as treatment—Control. Numbers in the figure are biomass in Control treatments. Stars above bars indicate significance of the treatment in each year, and stars next to text indicate a significant change in Control compared to 2009. Error bars are standard errors

3.4 | CO₂ flux responses to active layer thickness, water table, air temperature, and biomass

We evaluated the response of CO₂ fluxes to changes in ALT, WTD, chamber air temperatures, and plant biomass to determine whether these could explain the treatment effects and the variation observed through time. Ecosystem respiration and GPP both increased with

deeper ALT, higher plant biomass, and shallower WTD (wetter conditions) (Table 4). The response of GPP was always stronger than R_{eco} (larger coefficient values, Table 4). The interactions showed that the response of R_{eco} and GPP to ALT depended significantly on WTD, such that R_{eco} and GPP were suppressed at deep ALT when WTD was shallow (wetter conditions) ($\text{Reco}_{\text{alt}^* \text{wtd}}$: -122 to -52 ; $\text{GPP}_{\text{alt}^* \text{wtd}}$: -63 to -163 , Table 4). If biomass was high, however,

TABLE 4 Best predictor variables of R_{eco} , GPP, and NEE from multiple regression mixed effects models including active layer thickness (ALT), chamber temperature, plant biomass, and water table depth (WTD) at each plot

Response variable	Full model	Final variables	Coefficient	Min CI	Max CI	R ² Marginal	R ² Conditional	AIC
R_{eco} ($\text{g CO}_2 \text{ m}^{-2}$)	ALT*	Intercept	353.70	336.13	370.64	.32	.74	3193.95
	Biomass*	ALT	89.48	37.33	141.94			
	Chamber temperature*	Biomass	52.35	36.88	67.78			
	WTD	WTD	19.08	-2.10	41.05			
		ALT* WTD	-87.09	-122.20	-52.43			
		Biomass* WTD	61.51	25.75	97.84			
GPP ($\text{g CO}_2 \text{ m}^{-2}$)	ALT*	Intercept	455.71	433.31	478.76	.45	.77	3374.75
	Biomass*	ALT	135.84	55.35	216.12			
	Chamber temperature*	Biomass	119.00	95.13	141.84			
	WTD	WTD	19.68	-10.38	49.70			
		ALT* WTD	-112.96	-162.77	-63.06			
		Biomass* WTD	76.50	25.34	122.60			
NEE ($\text{g CO}_2 \text{ m}^{-2}$)	ALT*	Intercept	97.61	84.29	110.97	.23	.70	3107.41
	Biomass*	Biomass	69.96	56.98	83.28			
	Chamber temperature*	Chamber temp.	-21.00	-32.55	-9.21			
	WTD							

This analysis excludes data from 2009 (see Sections 2 and 4). All independent variables were standardized, and coefficients therefore represent effect size. Intercepts are in $\text{g CO}_2\text{-C m}^{-2}$. Bold values indicate significant effects. *indicates interaction terms; for the full model this means all interactions were initially included and for final variables only interaction terms that provided a significant model improvement were retained.

R_{eco} and GPP remained high in wet plots, regardless of thaw ($R_{\text{eco}}_{\text{biomass}^* \text{wtd}}$: 26–98; $\text{GPP}_{\text{biomass}^* \text{wtd}}$: 25–123, Table 4).

Net ecosystem exchange increased significantly with plant biomass and decreased with chamber temperature ($\text{NEE}_{\text{biomass}}$: 57–83; $\text{NEE}_{\text{chamber temp}}$: –33 to –9, Table 4). Net ecosystem exchange was not significantly related to ALT when other predictor variables were included in the model.

The models with combined environmental and plant biomass predictor variables explained 32% of R_{eco} , 45% of GPP, and 23% of NEE (marginal R^2 , Table 4), with additional plot-level variability that could not be explained by ALT, WTD, chamber temperature, and plant biomass (conditional R^2 , Table 4). After selecting the best model from ALT, WTD, chamber temperatures, and plant biomass, the residual analysis showed that treatments explained no additional variance in R_{eco} , GPP, or NEE.

The shape of the R_{eco} , GPP, and NEE relationship to ALT alone was best described by a single quadratic curve (Table 5), which captured the ALT*WTD interaction in the multiple parameter models (Figure 4). Ecosystem respiration and GPP increased during the initial stages of thaw, but leveled off or were slightly suppressed in deeply thawed, wet plots (Figure 4a,b). The quadratic fit between ALT and NEE was significant, and although ALT was not a significant predictor of NEE in the multiple parameter models, it was informative to investigate the shape of the relationship between ALT and NEE. The ALT and NEE relationship showed summer sink strength increased in the early stages of thaw, and became weaker in deeply thawed plots (Figure 4c).

3.5 | Seasonal CO₂ flux pattern

The seasonality of R_{eco} and GPP were both pronounced, with R_{eco} , GPP, and NEE peaks in mid-July (week 30) (Figure 5) and a net CO₂ sink from June to August of each year. At the beginning of each summer R_{eco} rates were similar (Figure 5a) and offset by GPP (Figure 5b) so that NEE was only a small source or neutral in May (Figure 5c). During May 2013 (week 18–21), the area was still snow-covered (Table 1), R_{eco} was low (Figure 5a, 2013), GPP was close to

TABLE 5 Model comparison of linear and quadratic active layer thickness and cumulative R_{eco} , GPP, and NEE, with and without treatment effects

Response variable	Full model	R^2		AIC
		Marginal	Conditional	
R_{eco}	ALT*Air*Soil	.28	.68	3288.4
	(ALT + ALT ²)*Air*Soil	.20	.81	3284.5
	(ALT + ALT ²)	.18	.78	3285.2
GPP	ALT*Air*Soil	.24	.71	3524.7
	(ALT + ALT ²)*Air*Soil	.19	.8	3517.0
	(ALT + ALT ²)	.21	.77	3510.3
NEE	ALT*Air*Soil	.11	.69	3207.1
	(ALT + ALT ²)*Air*Soil	.12	.73	3213.8
	(ALT + ALT ²)	.11	.73	3204.7

The best fitting model is shown in bold text.

zero (Figure 5b, 2013), and NEE was lower than in the other years (Figure 5c, 2013). Once the system was snow-free R_{eco} and GPP increased rapidly, and peak CO₂ fluxes were not suppressed or delayed by the late snowmelt.

At the end of the summer GPP declined more rapidly than R_{eco} , resulting in a late season net CO₂ source. The week of transition from sink to source at the end of the season was similar across years and treatments, with the exception of 2009 when all treatments transitioned to a source 2–3 weeks early due to declining GPP (Table 2, Figure 5).

3.6 | Early and late summer cumulative CO₂ fluxes

To evaluate the effect of warming treatments on early and late summer CO₂ flux dynamics, we calculated cumulative fluxes based on the most common week of source/sink transitions (Table 2). Early 2013 fluxes are shown for comparison with other years, but not included in the analysis because they were estimated using different models, and the data failed to meet model assumptions, even with transformation.

Early in the summer, R_{eco} and GPP were significantly higher in Soil from 2011 to 2012 for R_{eco} and Soil and Air & Soil warming in 2010 to 2012 for GPP (R_{eco} : Soil₂₀₁₁: 6%–65%; Soil₂₀₁₂: 3%–61%; GPP: Soil₂₀₁₀: 5%–82%; Soil₂₀₁₁: 29%–125%; Soil₂₀₁₂: 6%–84%; Air & Soil₂₀₁₁: –61% to –14%; Air & Soil₂₀₁₂: –55% to –3%; Figure 6a,b; Table S6a,b). In 2014 the effect of Soil warming on R_{eco} started to decline, but R_{eco} remained high in Air & Soil warming. Soil warming effects were significant in 2015, with decreased R_{eco} in Soil warming and increased R_{eco} in Air & Soil compared to Control (R_{eco} : Soil₂₀₁₅: –37% to –2%; Air & Soil₂₀₁₅: 2%–88%; Figure 6a, Table S3a). The patterns in GPP were similar to R_{eco} in 2014 and 2015, but not significant (Figure 6b, Table S6b). Air warming slightly increased R_{eco} and GPP from 2009 to 2012, but the effect was not significant (Figure 6a, b; Table S6a,b). In 2014 and 2015 R_{eco} tended to be lower in response to Air warming, but was significant only in 2015 (R_{eco} : Air₂₀₁₅: –36% to –2%). In contrast GPP increased with Air warming in 2014 and 2015 (Figure 6b; Table S6b), resulting in a slightly stronger net sink (Figure 6c; Table S6c), although the effects were not significant.

Control tundra R_{eco} and GPP showed no temporal trend early in the summer. However, in 2014 and 2015, both early snowmelt years (Table 1), R_{eco} and GPP were significantly higher than in other years (R_{eco} : 2014: 1%–37%; 2015: 7%–46%; GPP: 2014: 2%–50%; 2015: 11%–65%; Figure 6a,b). Net ecosystem exchange was neutral early in the summer, with no significant treatment or temporal trend, but tended toward a greater sink in 2014 and 2015 (Figure 6c; Table S6c).

Late summer R_{eco} was significantly higher in Soil and Air & Soil warming from 2011 to 2014, declined significantly in 2015 in Soil, but remained high in Air & Soil warming (Soil₂₀₁₁: 6%–160%; Soil₂₀₁₂: 11%–165%; Soil₂₀₁₃: 17%–174%; Soil₂₀₁₄: 2%–152%; Air & Soil₂₀₁₅: 11%–199%; Figure 6d, Table S3a). Air warming significantly increased late summer R_{eco} from 2009 to 2011 after which the effect of Air warming steadily diminished (Air₂₀₀₉: 3%–145%; Air₂₀₁₀:

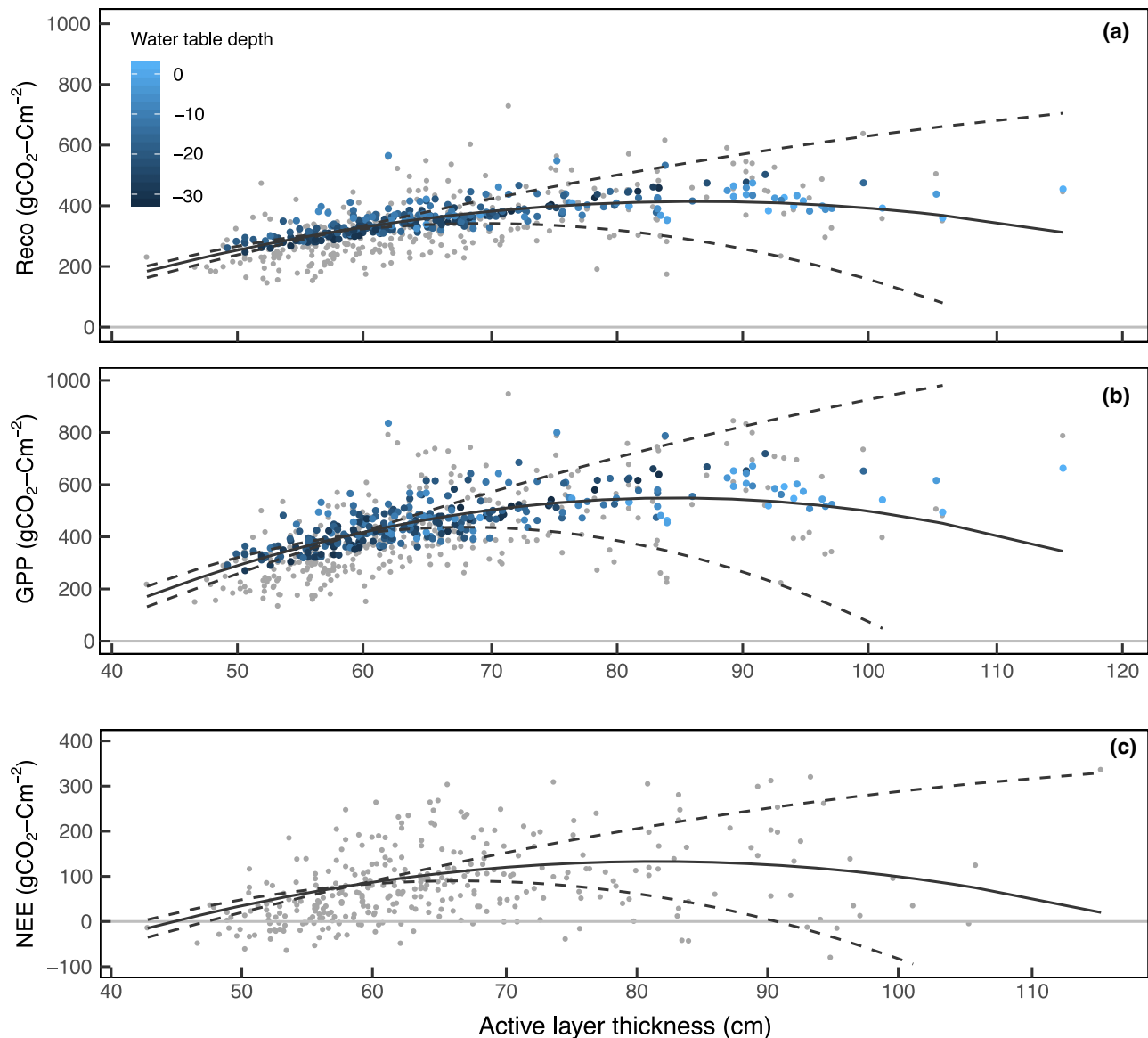


FIGURE 4 Response of cumulative R_{eco} (a), and gross primary productivity (GPP) (b), and net ecosystem CO_2 exchange (NEE) (c) to active layer thickness across all years and treatments. Gray dots show data, and colored dots show model predictions from multiple parameter models (Table 4), shaded by water table depth (dark = dry, light = wet); NEE has no shading because neither active layer thickness (ALT) nor water table depth (WTD) were significant predictors. Solid lines show the fit of the quadratic ALT response with 95% CI (dotted). Data from 2009 were excluded from the analyses (see Sections 2 and 4)

–22% to 116%; Air₂₀₁₁: –15% to 127%; Air₂₀₁₂: –25% to 112%; Air₂₀₁₃: –27% to 108%; Air₂₀₁₄: –30% to 104%; Air₂₀₁₅: –36% to 96%; Figure 6d, Table S6a). Gross primary productivity was typically lower than R_{eco} in the late summer with almost identical treatment responses as R_{eco} (Figure 6e, Table S6b). Net ecosystem exchange late in the summer was not significantly affected by treatments, except in 2014 when NEE was lower in Soil and Air & Soil warming treatments (Soil₂₀₁₄: –9% to –46%; Figure 6f, Table S6c), a trend that persisted in 2015.

In Control tundra, late summer R_{eco} and GPP from 2010 to 2015 were significantly higher than in 2009, but there was no directional trend through time (Figure 6d,e, Table S6a,b). Net ecosystem exchange was a consistent source in the late season, ranging from –11 to –24 g CO_2 m^{-2} , but the overall source strength did not

differ significantly from year to year (Figure 6f, Table S6c). In 2009, based on a common time period, late summer cumulative CO_2 fluxes were not significantly different from the other years, despite the early transition to a source (Table 2, Figure 5).

3.7 | Annual cumulative NEE

The tundra was either a net annual CO_2 source or net neutral across years, treatments, and estimation methods (Table 6). The CO_2 source was largest in 2009 (mean, Control₂₀₀₉: –170 g CO_2 m^{-2} ; Soil₂₀₀₉: –196 g CO_2 m^{-2} at the highest estimate, Table 6). Source strength declined from 2010 to 2013, with greater declines in Soil and Air & Soil warming than in Control and Air warming; the smallest CO_2 losses were in 2013 (Control₂₀₁₃: –105 g CO_2 m^{-2} ; Soil₂₀₁₃: –61 g

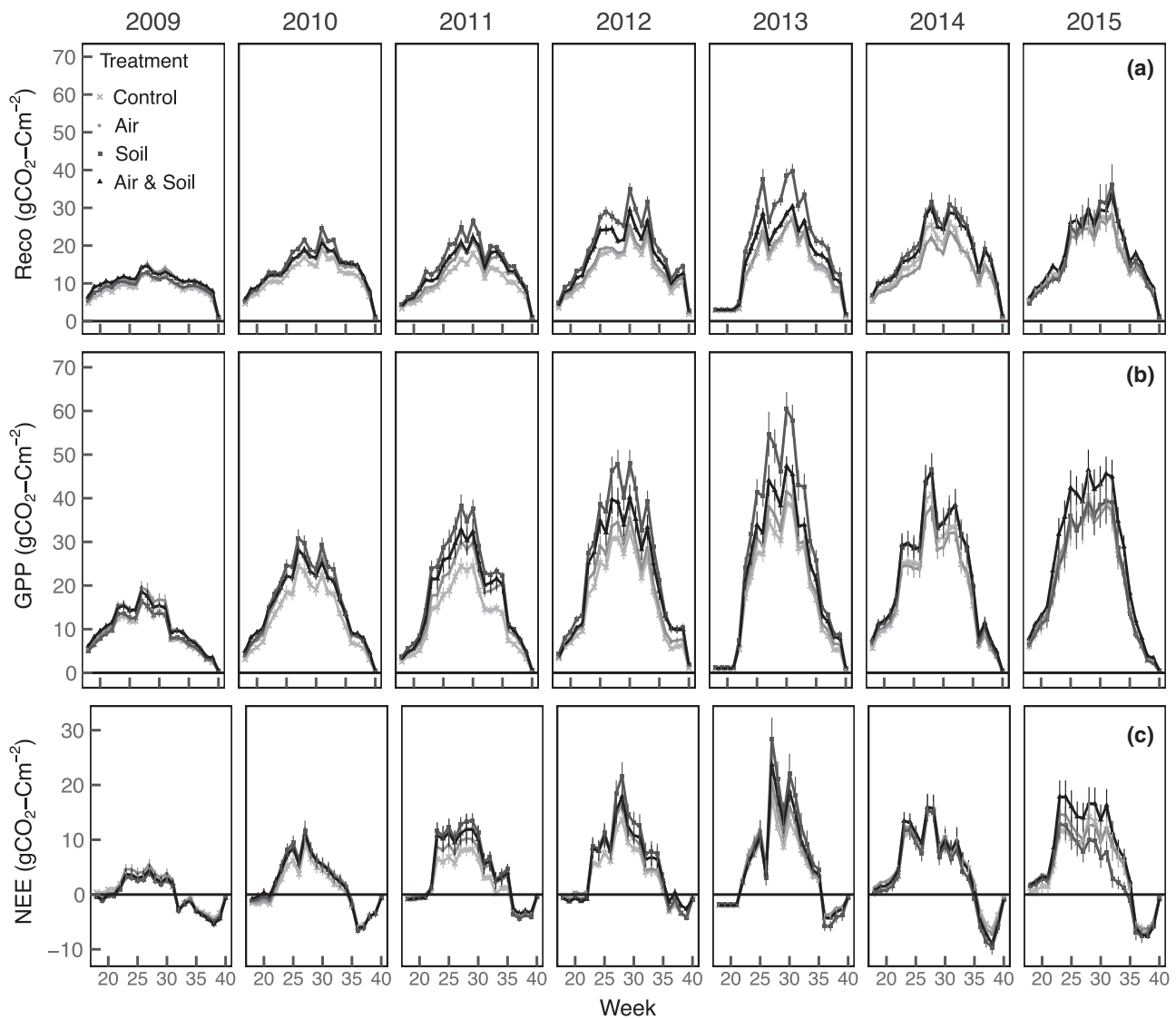


FIGURE 5 Summer pattern of average weekly cumulative R_{eco} (a), gross primary productivity (GPP) (b), and net ecosystem CO_2 exchange (NEE) (c) $\text{g CO}_2 \text{ m}^{-2}$ in each treatment and each year of measurement. Week 18 marks the first week of May, and week 40 marks the last week in September. In May 2013, a late snow fall year, CO_2 fluxes were estimated for the entire month using different methods (see Appendix S1), so we calculated average CO_2 flux/week for week 18–21 to illustrate the magnitude of CO_2 fluxes relative to other years. Positive values of NEE indicate a net CO_2 sink and negative values a source. Note the different scale for NEE. Error bars are standard error for that week

$\text{CO}_2 \text{ m}^{-2}$ at the high estimate, Table 6). In 2014 and 2015, the Soil (Soil_{2014} : $-123 \text{ g CO}_2 \text{ m}^{-2}$; Soil_{2015} : $-126 \text{ g CO}_2 \text{ m}^{-2}$ high estimate, Table 6) and Air & Soil treatment ($\text{Air \& Soil}_{2014}$: $-96 \text{ g CO}_2 \text{ m}^{-2}$; $\text{Air \& Soil}_{2015}$: $-44 \text{ g CO}_2 \text{ m}^{-2}$ at the high estimate, Table 6) once again were stronger annual net sources. In contrast annual CO_2 losses from Control and Air warming gradually decreased from 2010 onward, but remained either net neutral (low estimate) or a source (high estimate, Table 6).

4 | DISCUSSION

Over 7 years the effect of Soil warming on CO_2 fluxes was much stronger than Air warming. The different temporal responses in Soil,

Air & Soil, Air and Control could be explained by ALT, WTD, and plant biomass. In the initial stages of thaw R_{eco} and GPP increased linearly with ALT across all treatments resulting in a greater summer CO_2 sink. As ALT continued to increase in Soil and Air & Soil, saturated soil conditions caused R_{eco} and GPP to level off and summer CO_2 sink strength to decline. Summer CO_2 storage was offset by nonsummer CO_2 losses, in almost all years, but the size of the annual source depended on nonsummer estimation methods and strength of the summer sink. The rapid capacity of CO_2 fluxes to respond to thaw, and the similarity in CO_2 flux change per unit thaw across treatments, suggests that the results from rapid thaw are generalizable to ambient, yet slowly thawing, moist acidic tundra. The effect of permafrost thaw on CO_2 fluxes in the long term could not, however, be predicted from initial thaw stages, and surface soil

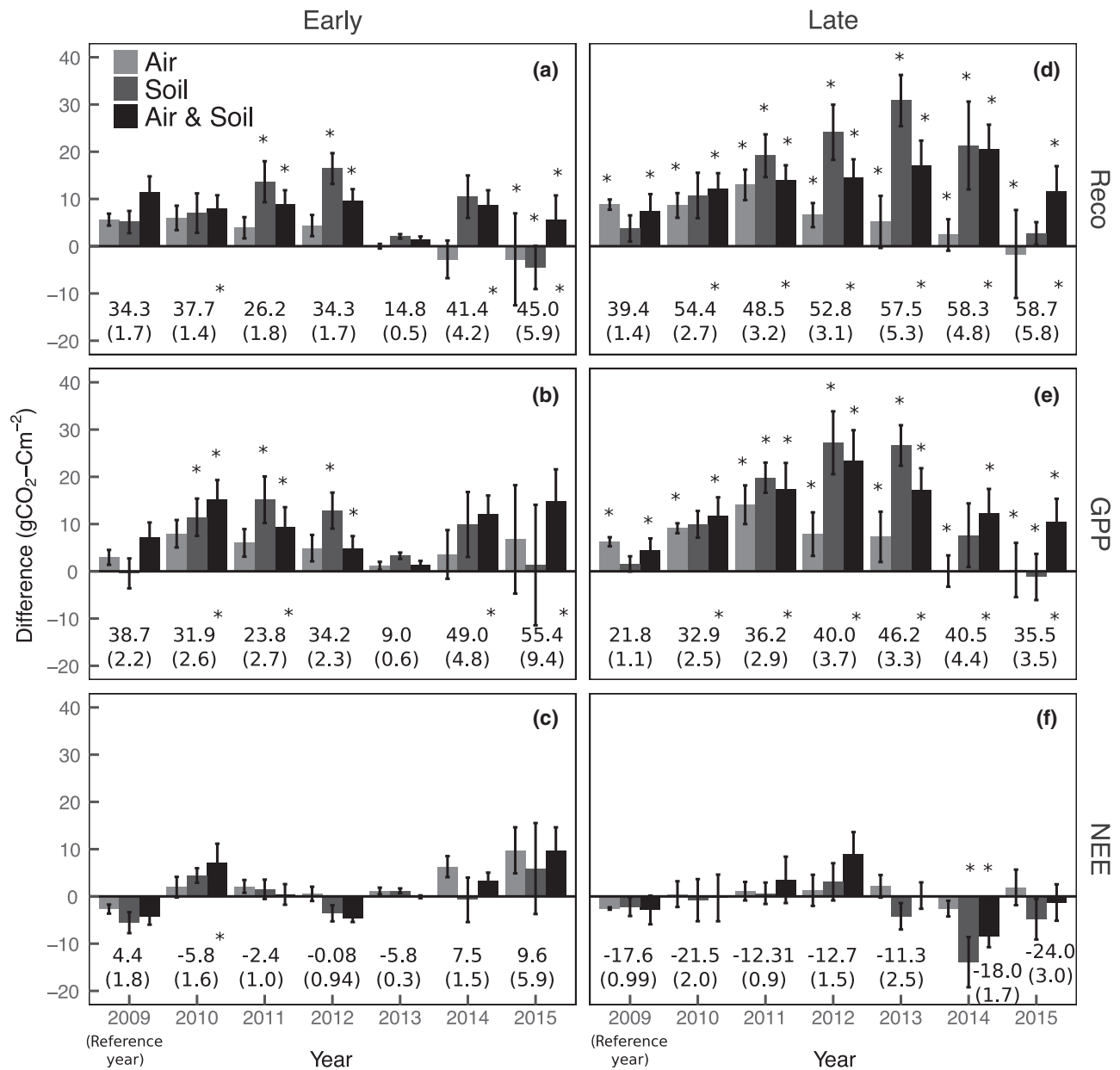


FIGURE 6 Difference in cumulative fluxes in early and late summer, calculated as treatment—Control. Early summer is the period before the system becomes a significant CO₂ sink for R_{eco} (a), gross primary productivity (GPP) (b), and net ecosystem CO₂ exchange (NEE) (c). Late summer is the period when the system has transitioned to a significant source for R_{eco} (d), GPP (e), and NEE (f). Numbers in the figure are cumulative fluxes for Control treatments. In May 2013, a late snow fall year, early CO₂ fluxes were estimated using different methods (see Appendix S1); cumulative early fluxes are shown for comparison, but not included in the statistical analysis. Stars above bars indicate significance of the treatment in each year, and stars next to text indicate a significant change in Control; all comparisons are relative to the reference year of 2009. Error bars are standard errors

moisture dynamics played an important role in the nonlinearity of the thaw response.

4.1 | Impact of warming treatments on environmental conditions

Deep winter Soil warming persisted into the summer after only two winters of warming (Natali et al., 2011), and after six winters unfrozen soil layers developed in Soil and Air & Soil warming (Table 1; Fig. S3). Active layer depth in Soil and Air & Soil deepened at rate of

6 cm/year, faster than ~3 cm/year observed at snow fences in Toolik, AK (Nowinski et al., 2010), possibly due to colder permafrost temperatures at the higher latitude (Osterkamp, Zhang, & Romanovsky, 1994). In Control and Air warming ALT increased ~2 cm/year. The rate of thaw in Control and Air warming may have been slightly accelerated by experimental infrastructure (e.g., boardwalks, data not shown), but not because of snow fence effects (Natali et al., 2011). Warming in Control tundra conforms to the warming trend in this part of Alaska (Panda, Marchenko, & Romanovsky, 2014) and falls within the range of ALT at a nearby site (Trucco et al., 2012). By 2100 ALT in this

TABLE 6 Annual CO₂ flux estimates based on the best-fit, non-summer R_{eco} estimate, and high R_{eco} estimate to reflect the lowest and highest range of losses

Year	Control		Air		Soil		Air & Soil	
	Low estimate	High estimate	Low estimate	High estimate	Low estimate	High estimate	Low estimate	High estimate
2009	-84 (9)	-178 (9)	-76 (14)	-170 (13)	-100 (9)	-196 (8)	-93 (16)	-189 (16)
2010	-57 (15)	-147 (15)	-34 (22)	-124 (22)	-39 (21)	-130 (21)	-40 (25)	-133 (25)
2011	-34 (15)	-124 (15)	-7 (26)	-97 (26)	6 (25)	-90 (25)	-4 (40)	-101 (40)
2012	-13 (17)	-108 (17)	8 (34)	-87 (34)	25 (31)	-73 (31)	12 (35)	-87 (35)
2013	-8 (16)	-105 (16)	15 (37)	-82 (37)	37 (34)	-61 (34)	19 (43)	-79 (43)
2014	5 (18)	-91 (18)	17 (35)	-80 (35)	-24 (27)	-123 (27)	3 (41)	-96 (41)
2015	9 (29)	-87 (29)	32 (42)	-64 (42)	-26 (35)	-126 (35)	56 (57)	-44 (57)

Negative values indicate a net CO₂ source, and positive values a net sink. Errors in parentheses are standard error.

region is expected to thaw beyond 1 m, extending up to 2.5 m (Koven et al., 2011; Panda et al., 2014). Thus thaw to 90 cm in Soil and Air & Soil warming represents half the expected ALT increase in the next century.

Air warming caused a consistent 0.4°C increase in daily average air temperature from May to September, with midday peaks frequently 2–4°C warmer and midday average temperatures 1°C higher (Natali et al., 2012). The daily average increases are smaller than the 1–3°C increases reported for other OTCs (Marion et al., 1997; Walker et al., 2006), but the midday temperatures are within range of these studies and projected Arctic warming of 2–4°C by 2100 (Collins et al., 2013; Koven et al., 2011).

Rapid thaw has caused the loss of soil ice structures (Plaza et al., submitted) and substantial ground surface subsidence in Soil and Air & Soil (M. Mauritz, personal observation). Subsidence has been most obvious in the last 2 years when water tables were frequently at or near the soil surface (Fig. S3). Ground surface subsidence and large variation in water table depth over small spatial scales are typical thermokarst features (Osterkamp et al., 2009) and have been documented at other snow fences (Blanc-Betes, Welker, Sturchio, Chanton, & Gonzalez-Meler, 2016; Hinkel & Hurd, 2006; Johansson et al., 2013). In coming years we expect more rapid thaw in wet areas as water increases the thermal capacity of soils (Romanovsky & Osterkamp, 2000), and with subsidence, the development of more extreme dry and wet microsites.

4.2 | Temporal trends of cumulative CO₂ fluxes

Air warming increased R_{eco} and GPP in the first summer (2009) (Natali et al., 2011), but was exceeded by the much larger effect of Soil warming after two winters (Natali et al., 2014). Over the next 5 years, the initial Air warming effect diminished and Air warming treatments generally behaved the same as Control. The weak response of CO₂ fluxes to Air warming was similar to other studies in tundra vegetation (Oberbauer et al., 2007; Shaver & Jonasson, 1999; Welker et al., 2004), and responses to higher soil nutrient availability are typically much stronger (Johnson et al., 2000; van Wijk et al., 2003). The rapid increase in CO₂ fluxes and plant biomass in Soil and Air & Soil support the hypothesis that C and N from

thawing permafrost contribute to plant productivity and ecosystem CO₂ loss (Harden et al., 2012; Keuper et al., 2012; Koven et al., 2015). In the first 5 years of warming R_{eco} , GPP, NEE were persistently lower in Air & Soil. The exact mechanisms of lower CO₂ fluxes in Air & Soil are unclear, but plant biomass and soil N concentrations were also lower compared to Soil warming (Salmon et al., 2016). This suggests biological, rather than environmental factors played a role because soil temperature, ALT, and water table dynamics were similar in Soil and Air & Soil treatments. Air & Soil warming effects were never significant, but the pattern indicates that the combined effects of warmer air temperatures and permafrost thaw were not additive.

After 5 years the patterns of all warming treatments shifted as the increase in R_{eco} , GPP, NEE, and plant biomass declined relative to Control in part due to gradual increases in the Control. The short-term, three-year response in Soil warming reflects the slower seven-year response in Control with similar magnitudes of increased R_{eco} (~40%), GPP (~50%), NEE (~500%), and biomass (~40%) (Figure 1; Tables 3, S3, S5). From 2010 to 2015 NEE in Control ranged from an average sink of 22 g CO₂ m⁻² in 2010 to 104 g CO₂ m⁻² in 2015, similar to NEE of other tundra sites in Alaska (Ueyama et al., 2013). Directional changes in experimental controls have been observed in other Arctic warming experiments (Wahren, Walker, & Bret-Harte, 2005) and match the trend of increased summer CO₂ storage with 30 years of warming across Arctic tundra (Belshe et al., 2013).

4.3 | Nonlinear CO₂ flux responses to thaw

The response of R_{eco} , GPP, and NEE to deepening ALT was best described by a single quadratic relationship, which captured the functional dependence on thaw, plant biomass, and water table dynamics. The response to ALT was similar across treatments in the initial stages of thaw from 55 to 75 cm, despite very different thaw rates in Soil and Air & Soil, Air and Control. Permafrost thaw from 55 to 75 cm increased soil C in the active layer by 70% (35–62 kg C m⁻²) and soil N by 62% (1.47–2.39 kg N m⁻²) (Plaza et al., submitted). Plants with roots near the permafrost table, such as sedges, are the most likely to benefit from N released during

permafrost thaw (Finger et al., 2016; Iversen et al., 2015; Keuper et al., 2012), and increased plant biomass at CiPEHR was dominated by *E. vaginatum* growth (Salmon et al., 2016). We found rapid increases in GPP as a function of thaw and biomass, and GPP was lower in plots with deep thaw and low biomass. This suggests that the capacity for greater CO₂ storage with thaw depends on plant community composition. Greater GPP in response to deeper thaw has been linked to *E. vaginatum* growth at other sites (Johansson et al., 2013; Malmer, Johansson, Olsrud, & Christensen, 2005; Schuur et al., 2007; Wahren et al., 2005), and *E. vaginatum* is among the first to grow with N fertilization (Chapin, Shaver, Giblin, Nadelhoffer, & Laundre, 1995). As thaw progressed, GPP leveled off, which could be a result of lower photosynthesis due to self-shading within a dense *E. vaginatum* canopy, or a transition toward greater shrub biomass (Street, Shaver, Williams, & Van Wijk, 2007), after the often transient growth response of *E. vaginatum* (Chapin et al., 1995; Hollister, Webber, & Tweedie, 2005; Wahren et al., 2005). From 2009 to 2013 there was no evidence for changes in plant community composition at CiPEHR (Salmon et al., 2016) and *E. vaginatum* can remain dominant if shrub biomass is initially low (Bret-Harte et al., 2008). The stabilization of total biomass at CiPEHR more likely reflects maximum growth capacity of *E. vaginatum* or, potentially, a shift from vegetative to reproductive growth (Arft et al., 1999), rather than a transition to shrub dominance. Dominant *E. vaginatum* has implications for ecosystem C balance in the longer term because, although *E. vaginatum* was linked to higher GPP, graminoids lack slow-decomposing woody biomass and promote faster ecosystem C and N turnover (DeMarco et al., 2014; Hobbie, 1996; Weintraub & Schimel, 2005), ultimately increasing C loss.

Increases in R_{eco} , with thaw, were most likely due to both greater autotrophic (R_a) and heterotrophic (R_h) respiration. Plant biomass was an important predictor in our multiple parameter R_{eco} models, and plant productivity and photosynthetic capacity in tundra ecosystems are generally correlated with R_{eco} (Boelman et al., 2003; Poyatos et al., 2014; Shaver et al., 2013). Even in the absence of thaw, GPP increases are accompanied by higher R_{eco} , which suggests that R_{eco} could increase primarily due to contributions from R_a (Hobbie & Chapin, 1998; Johnson et al., 2000; Shaver et al., 1998). Even with deeper thaw, isotopic flux partitioning studies have found that R_{eco} is often dominated by R_a (Hicks Pries, Logtestijn, et al., 2015). Increases in R_a , with thaw, are consistent with strong *E. vaginatum* growth (Salmon et al., 2016) and substantial contributions of *E. vaginatum* root and shoot respiration to total R_{eco} (Segal & Sullivan, 2014).

Ecosystem respiration also comprises decomposing soil C, and deep, old soil C losses increase with permafrost thaw (Hicks Pries, Schuur, & Crummer, 2013; Schuur et al., 2009) even while GPP offsets R_{eco} to create a net CO₂ sink in summer (Trucco et al., 2012). Higher plant productivity with deeper thaw initially increased NEE in Soil and Air & Soil. The relationship between greater NEE with higher biomass is to be expected, but it suggests that the effect on net summer CO₂ balance depends more on rapid plant growth with ALT than on greater soil decomposition and loss via R_{eco} . NEE

peaked in the third year, declining after 2011 as the proportion of R_{eco} increased relative to GPP (Figure 2; Table 3). The initial increase, and then decline in NEE with Soil and Air & Soil, appears to be due to a lag in R_{eco} and suggests that the R_h contribution to thaw may have increased more gradually as thaw deepened and the soil column warmed. A partitioning study at CiPEHR found that thaw increased loss of deep, old soil C by 6%–44% (Hicks Pries, Schuur, et al., 2016); thus, R_h increases were of similar magnitude as the 30%–40% higher R_{eco} in Soil warming from 2011 to 2013 (Table 3).

4.4 | Soil moisture dynamics and CO₂ flux

Soil moisture was an important factor in the CO₂ flux response to thaw. Deep thaw created consistently wetter soil conditions as the ground surface subsided, and in the last 2 years a number of microsites had water at or above the ground surface (Fig. S3). Saturated soil surface conditions caused lower R_{eco} , GPP, and NEE than we would have expected based on the initial linear thaw trajectory with dry surface soils. The long-term trajectory for upland Arctic ecosystems is toward drier conditions as permafrost recedes into the ground and water drains (Avis et al., 2011). However, intermediate stages of thaw can lead to wetter or completely saturated microsites as the ground surface subsides and permafrost prevents drainage (Jorgenson et al., 2013; Osterkamp et al., 2009).

We found that water table position changed the trajectory of CO₂ fluxes based on initial linear increases under dry conditions. Deep thaw, subsidence, and flooding coincided with two very wet years (2014 and 2015); despite an overall higher water table, surface soils were not saturated in Control and Air warming, and R_{eco} and GPP continued to increase with thaw. In contrast, the most deeply thawed areas were also the wettest, which suppressed R_{eco} , GPP, and NEE. As long as the soil column does not become completely saturated, increases in soil moisture can stimulate decomposition (Hicks Pries, Schuur, Vogel, & Natali, 2013) and R_{eco} (Euskirchen, Edgar, Turetsky, Waldrop, & Harden, 2014; Euskirchen et al., 2012), but reduced plant water stress also stimulates GPP and can increase net CO₂ uptake (Chivers et al., 2009; Nobrega & Grogan, 2008; Sjögersten, van der Wal, & Woodin, 2006; Tuittila, Vasander, & Laine, 2004). Standing water table, on the other hand, limits oxygen availability, lowering R_{eco} , and GPP and can create a net summer ecosystem CO₂ source (Euskirchen, Edgar, et al., 2014; Welker et al., 2004; Zona et al., 2009). We found that the effect of high water table on R_{eco} and GPP also depended on plant biomass, and the tolerance of *E. vaginatum* to wet conditions may have sustained high GPP (Johnson et al., 1996) and R_a , even under flooded conditions. The strong response of R_{eco} to soil surface flooding highlights that a large proportion of R_{eco} must come from R_a and R_h in surface soils (McConnell et al., 2013).

The trajectory of ecosystem C storage in deeply thawed moist acidic tundra will be highly dependent on water table dynamics. Although anaerobic conditions can continue to limit soil C loss even after permafrost thaws (Elberling et al., 2013), we found that GPP

declined more rapidly than R_{eco} , and CO_2 losses are likely to be greatest in subsided areas. The majority of current plant species will not tolerate complete submergence, and senescence will produce a pulse of litter, increasing CO_2 losses from wet sites. Wetter soil conditions in the Soil warmed plots enhanced CH_4 emission at CiPEHR (Natali et al., 2015) and were not quantified in this study, but are likely to increase further in subsided areas and are the subject of future investigation. Soil drying is expected to cause greater CO_2 loss and decomposition of old soil C as permafrost continues to recede (Natali et al., 2015), due to higher microbial decomposition in aerobic conditions and lower GPP, as plants become drought stressed (Euskirchen, Edgar, et al., 2014; Nobrega & Grogan, 2008; Oechel et al., 1993; Sjögersten et al., 2006). Continued monitoring will be important to understand the complex role of soil moisture on C balance, as thaw progresses.

4.5 | Early and late season CO_2 flux dynamics

The effect of Arctic warming and permafrost thaw on C balance will depend critically on how plants and microbes respond to warming in different parts of the year (Euskirchen, Carman, & McGuire, 2014). Removal of excess snow ensured similar growing season length across experimental treatments (Table 1), but bud-break occurred 2–5 days earlier in Soil and Air & Soil (Natali et al., 2012). Early season GPP was significantly higher in Soil and Air & Soil and suggests that mechanisms other than air temperature, such as greater plant N uptake in warm winter soils (Bosiö et al., 2014; Leffler & Welker, 2013), might also stimulate early CO_2 uptake. Increased GPP did not affect early season NEE due to concurrent increases in R_{eco} . Across all treatments the timing of snowmelt exerted strong control on early season CO_2 fluxes. Net CO_2 uptake was high in 2014 and 2015, two very low snowfall and early snowmelt years. In contrast late snowmelt in 2013 produced low GPP and lower NEE early in the season. However, late snowmelt did not reduce peak GPP or NEE during the 2013 summer (Figure 5), contrary to other studies (Aurela et al., 2004; Euskirchen et al., 2012), presumably because *E. vaginatum* photosynthetic activity can increase rapidly after snow melts (Fahnestock et al., 1999), and high snow conditions enhance *E. vaginatum* productivity (Johansson et al., 2013; Walker et al., 1999).

Late summer CO_2 fluxes are important because R_{eco} after plants have senesced can shift tundra to an annual net CO_2 sink (Euskirchen et al., 2012; Ueyama et al., 2014). Late summer R_{eco} was 25%–40% higher in Soil and Air & Soil (Table S6a), but was offset by higher GPP, consistent with delayed senescence (Natali et al., 2012). High productivity during the summer creates a stronger CO_2 sink, but can also enhance winter CO_2 losses by increasing labile C substrate availability (Grogan & Jonasson, 2005; Larsen et al., 2007). Warm winter soils continued to increase R_{eco} and cumulative non-summer losses exceed summer CO_2 uptake resulting in a net CO_2 source of up to $126 \text{ g CO}_2\text{-C m}^{-2}$. High net CO_2 uptake in well-drained Control and Air warming treatments during the summer season and cooler winter soil temperatures created a much smaller annual net source (Table 6). At the nearby thaw gradient site Trucco

et al. (2012) similarly found that in the initial stages of thaw, where *E. vaginatum* was dominant, and soils were well drained, summer season CO_2 uptake exceeded winter losses. We suspect that losses in Soil and Air & Soil in 2014 and 2015 may have been higher than predicted by the temperature-driven models due to unfrozen soil layers and greater soil moisture in areas with greater thaw (Welker et al., 2004). Winter estimates of CO_2 loss completely changed the interpretation of how permafrost thaw impacts ecosystem CO_2 storage. Winter remains the most uncertain period due to poorly predictable flux rates and sparse data, but is critical to truly quantify Arctic contributions to global atmospheric greenhouse gas concentrations. A coordinated and replicated series of experiments that stimulate permafrost thaw across a range of ecosystem types, and hydrologic regimes, similar to the ITEX network, and include year-round monitoring, would provide crucial insight to the effect of permafrost thaw on C storage across the Arctic.

ACKNOWLEDGEMENTS

We would like to thank J. Ledman, numerous invaluable field technicians, and the staff at Bonanza Creek LTER for continued field and logistical support. This project would not be possible without their help. The NAU statistical consulting lab and discussions with C. Plaza advanced the analysis of this data set. Funding for this research was provided by: U.S. Department of Energy, Office of Biological and Environmental Research, Terrestrial Ecosystem Science (TES) Program; National Science Foundation CAREER program; National Parks Inventory and Monitoring Program; National Science Foundation Bonanza Creek LTER program.

REFERENCES

- Abbott, B. W., Jones, J. B., Schuur, E. A. G., Chapin, F. S. III, Bowden, W. B., Bret-Harte, M. S., ... Zimov, S. (2016). Biomass offsets little or none of permafrost carbon release from soils, streams, and wildfire: An expert assessment. *Environmental Research Letters*, *11*, 034014.
- Aerts, R., Cornelissen, J. H. C., & Dorrepaal, E. (2006). Plant performance in a warmer world: General responses of plants from cold, northern biomes and the importance of winter and spring events. *Plant Ecology*, *182*, 65–77.
- Arft, A. M., Walker, M. D., Gurevitch, J., Alatalo, J. M., Bret-Harte, M. S., Dale, M., ... Wookey, P. A. (1999). Responses of tundra plants to experimental warming: Meta-analysis of the international tundra experiment. *Ecological Monographs*, *69*, 491–511.
- Aurela, M., Laurila, T., & Tuovinen, J. P. (2004). The timing of snow melt controls the annual CO_2 balance in a subarctic fen. *Geophysical Research Letters*, *31*, L16119.
- Avis, C. A., Weaver, A. J., & Meissner, K. J. (2011). Reduction in areal extent of high-latitude wetlands in response to permafrost thaw. *Nature Geoscience*, *4*, 444–448.
- Barr, D. J., Levy, R., Scheepers, C., & Tily, H. J. (2013). Random effects structure for confirmatory hypothesis testing: Keep it maximal. *Journal of Memory and Language*, *68*, 255–278.
- Bartón, K. (2016). *Multi-Model Inference (MuMIn)*.
- Bates, D., Mächler, M., Bolker, B., & Walker, S. (2015). Fitting linear mixed-effects models using lme4. *Journal of Statistical Software*, *1(1)*, 2015.

- Belshe, E. F., Schuur, E. A. G., & Bolker, B. M. (2013). Tundra ecosystems observed to be CO₂ sources due to differential amplification of the carbon cycle. *Ecology Letters*, *16*, 1307–1315.
- Belshe, E., Schuur, E., Bolker, B., & Bracho, R. (2012). Incorporating spatial heterogeneity created by permafrost thaw into a landscape carbon estimate. *Journal of Geophysical Research-Biogeosciences*, *117*, G01026.
- Blanc-Betes, E., Welker, J. M., Sturchio, N. C., Chanton, J. P., & Gonzalez-Meler, M. A. (2016). Winter precipitation and snow accumulation drive the methane sink or source strength of Arctic tussock tundra. *Global Change Biology*, *22*, 2818–2833.
- Boelman, N. T., Stieglitz, M., Rueth, H. M., Sommerkorn, M., Griffin, K. L., Shaver, G. R., & Gamon, J. A. (2003). Response of NDVI, biomass, and ecosystem gas exchange to long-term warming and fertilization in wet sedge tundra. *Oecologia*, *135*, 414–421.
- Bosio, J., Stiegler, C., Johansson, M., Mbufong, H. N., & Christensen, T. R. (2014). Increased photosynthesis compensates for shorter growing season in subarctic tundra—8 years of snow accumulation manipulations. *Climatic Change*, *127*, 321–334.
- Bret-Harte, M. S., Mack, M. C., Goldsmith, G. R., Sloan, D. B., DeMarco, J., Shaver, G. R., ... Chapin, F. S. (2008). Plant functional types do not predict biomass responses to removal and fertilization in Alaskan tussock tundra. *Journal of Ecology*, *96*, 713–726.
- Celis, G., Mauritz, M., Bracho, R., Salmon, S., Webb, E. E., Hutchings, J., ... Schuur, E. A. G. Tundra is a consistent source of CO₂ at a site with progressive permafrost thaw during six years of chamber and eddy covariance measurements. *Journal of Geophysical Research: Biogeosciences*. in review.
- Chapin, F. S. III (1983). Direct and indirect effects of temperature on arctic plants. *Polar Biology*, *2*, 47–52.
- Chapin, F. S. III, Shaver, G. R., Giblin, A. E., Nadelhoffer, K. G., & Laundre, J. A. (1995). Response of arctic tundra to experimental and observed changes in climate. *Ecology*, *76*, 694–711.
- Chivers, M. R., Turetsky, M. R., Waddington, J. M., Harden, J. W., & McGuire, A. D. (2009). Effects of experimental water table and temperature manipulations on ecosystem CO₂ fluxes in an Alaskan rich fen. *Ecosystems*, *12*, 1329–1342.
- Collins, M., Knutti, R., Arblaster, J., Dufresne, J.-L., Fichefet, T., Friedlingstein, P., ... Wehner, M. (2013). *Long-term climate change: Projections, commitments and irreversibility*. Cambridge, United Kingdom and New York, NY: Cambridge University Press.
- Deane-Coe, K. K., Mauritz, M., Celis, G., Salmon, V., Crummer, K. G., Natali, S. M., & Schuur, E. A. G. (2015). Experimental warming alters productivity and isotopic signatures of tundra mosses. *Ecosystems*, *18*, 1070–1082.
- DeMarco, J., Mack, M. C., Bret-Harte, M. S., Burton, M., & Shaver, G. R. (2014). Long-term experimental warming and nutrient additions increase productivity in tall deciduous shrub tundra. *Ecosphere*, *5*, 72.
- Dorrepaal, E., Toet, S., van Logtestijn, R. S. P., Swart, E., van de Weg, M. J., Callaghan, T. V., & Aerts, R. (2009). Carbon respiration from sub-surface peat accelerated by climate warming in the subarctic. *Nature*, *460*, 616–U679.
- Elberling, B., Michelsen, A., Schadel, C., Schuur, E. A. G., Christiansen, H. H., Berg, L., ... Sigsgaard, C. (2013). Long-term CO₂ production following permafrost thaw. *Nature Climate Change*, *3*, 890–894.
- Elmendorf, S. C., Henry, G. H. R., Hollister, R. D., Fosaa, A. M., Gould, W. A., Hermanutz, L., ... Walker, M. D. (2015). Experiment, monitoring, and gradient methods used to infer climate change effects on plant communities yield consistent patterns. *Proceedings of the National Academy of Sciences*, *112*, 448–452.
- Euskirchen, E. S., Bret-Harte, M. S., Scott, G. J., Edgar, C., & Shaver, G. R. (2012). Seasonal patterns of carbon dioxide and water fluxes in three representative tundra ecosystems in northern Alaska. *Ecosphere*, *3*, 4.
- Euskirchen, E. S., Carman, T. B., & McGuire, A. D. (2014). Changes in the structure and function of northern Alaskan ecosystems when considering variable leaf-out times across groupings of species in a dynamic vegetation model. *Global Change Biology*, *20*, 963–978.
- Euskirchen, E. S., Edgar, C. W., Turetsky, M. R., Waldrop, M. P., & Harden, J. W. (2014). Differential response of carbon fluxes to climate in three peatland ecosystems that vary in the presence and stability of permafrost. *Journal of Geophysical Research: Biogeosciences*, *119*, 1576–1595.
- Fahnestock, J. T., Jones, M. H., & Welker, J. M. (1999). Wintertime CO₂ efflux from arctic soils: Implications for annual carbon budgets. *Global Biogeochemical Cycles*, *13*, 775–779.
- Finger, R. A., Turetsky, M. R., Kielland, K., Ruess, R. W., Mack, M. C., & Euskirchen, E. S. (2016). Effects of permafrost thaw on nitrogen availability and plant–soil interactions in a boreal Alaskan lowland. *Journal of Ecology*, *104*, 1542–1554.
- Grogan, P., & Jonasson, S. (2005). Temperature and substrate controls on intra-annual variation in ecosystem respiration in two subarctic vegetation types. *Global Change Biology*, *11*, 465–475.
- Harden, J., Koven, C., Ping, C., Hugelius, G., McGuire, A., Camill, P., ... Grosse, G. (2012). Field information links permafrost carbon to physical vulnerabilities of thawing. *Geophysical Research Letters*, *39*, L15704.
- Hicks Pries, C. E., Logtestijn, R. S., Schuur, E. A., Natali, S. M., Cornelissen, J. H., Aerts, R., & Dorrepaal, E. (2015). Decadal warming causes a consistent and persistent shift from heterotrophic to autotrophic respiration in contrasting permafrost ecosystems. *Global Change Biology*, *21*, 4508–4519.
- Hicks Pries, C. E., Schuur, E. A. G., & Crummer, K. G. (2013). Thawing permafrost increases old soil and autotrophic respiration in tundra: Partitioning ecosystem respiration using $\delta^{13}\text{C}$ and $\Delta^{14}\text{C}$. *Global Change Biology*, *19*, 649–661.
- Hicks Pries, C. E., Schuur, E. A. G., Natali, S. M., & Crummer, K. G. (2016). Old soil carbon losses increase with ecosystem respiration in experimentally thawed tundra. *Nature Climate Change*, *6*, 214–218.
- Hicks Pries, C. E., Schuur, E. A. G., Vogel, J. G., & Natali, S. M. (2013). Moisture drives surface decomposition in thawing tundra. *Journal of Geophysical Research: Biogeosciences*, *118*, 1133–1143.
- Hinkel, K. M., & Hurd, J. K. (2006). Permafrost destabilization and thermokarst following snow fence installation, Barrow, Alaska, USA. *Arctic Antarctic and Alpine Research*, *38*, 530–539.
- Hobbie, S. E. (1996). Temperature and plant species control over litter decomposition in Alaskan tundra. *Ecological Monographs*, *66*, 503–522.
- Hobbie, S. E., & Chapin, F. S. III (1998). The response of tundra plant biomass, aboveground production, nitrogen, and CO₂ flux to experimental warming. *Ecology*, *79*, 1526–1544.
- Hobbie, S. E., Nadelhoffer, K. J., & Hogberg, P. (2002). A synthesis: The role of nutrients as constraints on carbon balances in boreal and arctic regions. *Plant and Soil*, *242*, 163–170.
- Hollister, R. D., Webber, P. J., & Tweedie, C. E. (2005). The response of Alaskan arctic tundra to experimental warming: Differences between short- and long-term responses. *Global Change Biology*, *11*, 525–536.
- Hugelius, G., Strauss, J., Zubrzycki, S., Harden, J. W., Schuur, E. A. G., Ping, C. L., ... Kuhry, P. (2014). Estimated stocks of circumpolar permafrost carbon with quantified uncertainty ranges and identified data gaps. *Biogeosciences*, *11*, 6573–6593.
- Iversen, C. M., Sloan, V. L., Sullivan, P. F., Euskirchen, E. S., McGuire, A. D., Norby, R. J., ... Wulfschleger, S. D. (2015). The unseen iceberg: Plant roots in arctic tundra. *New Phytologist*, *205*, 34–58.
- Johansson, M., Callaghan, T. V., Bosio, J., Åkerman, H. J., Jackowicz-Korczynski, M., & Christensen, T. R. (2013). Rapid responses of permafrost and vegetation to experimentally increased snow cover in sub-arctic Sweden. *Environmental Research Letters*, *8*, 035025.

- Johnson, P. C. D. (2014). Extension of Nakagawa & Schielzeth's R(2) (GLMM) to random slopes models. *Methods in Ecology and Evolution*, 5, 944–946.
- Johnson, L. C., Shaver, G. R., Cades, D. H., Rastetter, E., Nadelhoffer, K., Giblin, A., ... Stanley, A. (2000). Plant carbon-nutrient interactions control CO₂ exchange in Alaskan wet sedge tundra ecosystems. *Ecology*, 81, 453–469.
- Johnson, L. C., Shaver, G. R., Giblin, A. E., Nadelhoffer, K. J., Rastetter, E. R., Laundre, J. A., & Murray, G. L. (1996). Effects of drainage and temperature on carbon balance of tussock tundra microcosms. *Oecologia*, 108, 737–748.
- Jorgenson, M. T., Harden, J., Kanevskiy, M., Jonathan, O., Wickland, K., Ewing, S., ... Striegl, R. (2013). Reorganization of vegetation, hydrology and soil carbon after permafrost degradation across heterogeneous boreal landscapes. *Environmental Research Letters*, 8, 035017.
- Jorgenson, M. T., Racine, C. H., Walters, J. C., & Osterkamp, T. E. (2001). Permafrost degradation and ecological changes associated with a warming climate in central Alaska. *Climatic Change*, 48, 551–579.
- Keuper, F., van Bodegom, P. M., Dorrepaal, E., Weedon, J. T., van Hal, J., van Logtestijn, R. S. P., & Aerts, R. (2012). A frozen feast: Thawing permafrost increases plant-available nitrogen in subarctic peatlands. *Global Change Biology*, 18, 1998–2007.
- Köchy, M., Hiederer, R., & Freibauer, A. (2015). Global distribution of soil organic carbon – Part 1: Masses and frequency distributions of SOC stocks for the tropics, permafrost regions, wetlands, and the world. *Soil*, 1, 351–365.
- Koven, C. D., Lawrence, D. M., & Riley, W. J. (2015). Permafrost carbon–climate feedback is sensitive to deep soil carbon decomposability but not deep soil nitrogen dynamics. *Proceedings of the National Academy of Sciences of the United States of America*, 112, 3752–3757.
- Koven, C., Ringeval, B., Friedlingstein, P., Ciais, P., Cadule, P., Khvorostyanov, D., ... Tarnocai, C. (2011). Permafrost carbon-climate feedbacks accelerate global warming. *Proceedings of the National Academy of Sciences*, 108, 14769–14774.
- Larsen, K. S., Grogan, P., Jonasson, S., & Michelsen, A. (2007). Respiration and microbial dynamics in two subarctic ecosystems during winter and spring thaw: Effects of increased snow depth. *Arctic, Antarctic, and Alpine Research*, 39, 268–276.
- Leffler, J. A., & Welker, J. M. (2013). Long-term increases in snow pack elevate leaf N and photosynthesis in *Salix arctica*: Responses to a snow fence experiment in the High Arctic of NW Greenland. *Environmental Research Letters*, 8, 025023.
- Liljedahl, A. K., Boike, J., Daanen, R. P., Fedorov, A. N., Frost, G. V., Grosse, G., ... Zona, D. (2016). Pan-Arctic ice-wedge degradation in warming permafrost and its influence on tundra hydrology. *Nature Geoscience*, 9, 312–318.
- Mack, M. C., Schuur, E. A. G., Bret-Harte, M. S., Shaver, G. R., & Chapin, F. S. (2004). Ecosystem carbon storage in arctic tundra reduced by long-term nutrient fertilization. *Nature*, 431, 440–443.
- Malmer, N., Johansson, T., Olsrud, M., & Christensen, T. R. (2005). Vegetation, climatic changes and net carbon sequestration in a North-Scandinavian subarctic mire over 30 years. *Global Change Biology*, 11, 1895–1909.
- Marion, G. M., Henry, G. H. R., Freckman, D. W., Johnstone, J., Jones, G., Jones, M. H., ... Virginia, R. A. (1997). Open-top designs for manipulating field temperature in high-latitude ecosystems. *Global Change Biology*, 3, 20–32.
- McConnell, N. A., Turetsky, M. R., McGuire, A. D., Kane, E. S., Waldrop, M. P., & Harden, J. W. (2013). Controls on ecosystem and root respiration across a permafrost and wetland gradient in interior Alaska. *Environmental Research Letters*, 8, 045029.
- McGuire, A., Christensen, T., Hayes, D., Heroult, A., Euskirchen, E., Kimball, J., ... Yi, Y. (2012). An assessment of the carbon balance of Arctic tundra: Comparisons among observations, process models, and atmospheric inversions. *Biogeosciences*, 9, 3185–3204.
- McGuire, A. D., Koven, C., Lawrence, D. M., Clein, J. S., Xia, J., Beer, C., & Zhuang, Q. (2016). Variability in the sensitivity among model simulations of permafrost and carbon dynamics in the permafrost region between 1960 and 2009. *Global Biogeochemical Cycles*, 30, 1015–1037.
- Nadelhoffer, K. J., Giblin, A. E., Shaver, G. R., & Laundre, J. A. (1991). Effects of temperature and substrate quality on element mineralization in six arctic soils. *Ecology*, 72, 242–253.
- Nakagawa, S., & Schielzeth, H. (2013). A general and simple method for obtaining R² from generalized linear mixed-effects models. *Methods in Ecology and Evolution*, 4, 133–142.
- Natali, S. M., Schuur, E. A. G., Mauritz, M., Schade, J., Celis, G., Crummer, G., ... Salmon, V. (2015). Permafrost thaw and soil moisture drive CO₂ and CH₄ release from upland tundra. *Journal of Geophysical Research, Biogeosciences*, 120, 525–537.
- Natali, S., Schuur, E., & Rubin, R. (2012). Increased plant productivity in Alaskan tundra as a result of experimental warming of soil and permafrost. *Journal of Ecology*, 100, 488–498.
- Natali, S., Schuur, E., Trucco, C., Pries, C., Crummer, K., & Lopez, A. (2011). Effects of experimental warming of air, soil and permafrost on carbon balance in Alaskan tundra. *Global Change Biology*, 17, 1394–1407.
- Natali, S. M., Schuur, E. A. G., Webb, E. E., Pries, C. E. H., & Crummer, K. G. (2014). Permafrost degradation stimulates carbon loss from experimentally warmed tundra. *Ecology*, 95, 602–608.
- Nobrega, S., & Grogan, P. (2008). Landscape and ecosystem-level controls on net carbon dioxide exchange along a natural moisture gradient in Canadian low arctic tundra. *Ecosystems*, 11, 377–396.
- Nowinski, N. S., Taneva, L., Trumbore, S. E., & Welker, J. M. (2010). Decomposition of old organic matter as a result of deeper active layers in a snow depth manipulation experiment. *Oecologia*, 163, 785–792.
- Oberbauer, S. F., Tweedie, C. E., Welker, J. M., Fahnestock, J. T., Henry, G. H. R., Webber, P. J., ... Starr, G. (2007). Tundra CO₂ fluxes in response to experimental warming across latitudinal and moisture gradients. *Ecological Monographs*, 77, 221–238.
- O'Donnell, J., Jorgenson, M., Harden, J., McGuire, A., Kanevskiy, M., & Wickland, K. (2012). The effects of permafrost thaw on soil hydrologic, thermal and carbon dynamics in an Alaskan peatland. *Ecosystems*, 15, 213–229.
- Oechel, W. C., Hastings, S. J., Vourlitis, G., Jenkins, M., Riechers, G., & Grulke, N. (1993). Recent change of Arctic tundra ecosystems from a net carbon dioxide sink to a source. *Nature*, 361, 520–523.
- Oechel, W. C., Laskowski, C. A., Burba, G., Gioli, B., & Kalhori, A. A. M. (2014). Annual patterns and budget of CO₂ flux in an Arctic tussock tundra ecosystem. *Journal of Geophysical Research: Biogeosciences*, 119, 323–339.
- Oechel, W. C., Vourlitis, G. L., Hastings, S. J., Ault, R. P., & Bryant, P. (1998). The effects of water table manipulation and elevated temperature on the net CO₂ flux of wet sedge tundra ecosystems. *Global Change Biology*, 4, 77–90.
- Osterkamp, T. E., Jorgenson, M. T., Schuur, E. A. G., Shur, Y. L., Kanevskiy, M. Z., Vogel, J. G., & Tumskey, V. E. (2009). Physical and ecological changes associated with warming permafrost and thermokarst in interior Alaska. *Permafrost and Periglacial Processes*, 20, 235–256.
- Osterkamp, T. E., Zhang, T., & Romanovsky, V. E. (1994). Thermal regime of permafrost in Alaska and predicted global warming. *Journal of Cold Regions Engineering*, 4, 38–42.
- Overland, J., Hanna, E., Hanssen-Bauer, I., Kim, S. J., Walsh, J. E., Wang, M., ... Thoman, R. L. (2016). *Air Temperature [in Arctic Report Card 2016]*. Retrieved from <http://www.arctic.noaa.gov/reportcard>
- Panda, S. K., Marchenko, S. S., & Romanovsky, V. E. (2014). High-resolution permafrost modeling in Denali National Park and Preserve. Natural Resource Technical Report NPS/CAKN/NRTR 2014/858. Fort Collins, CO: National Park Service.

- Patrick, L. D., Ogle, K., Bell, C. W., Zak, J., & Tissue, D. (2009). Physiological responses of two contrasting desert plant species to precipitation variability are differentially regulated by soil moisture and nitrogen dynamics. *Global Change Biology*, *15*, 1214–1229.
- Ping, C., Jastrow, J., Jorgenson, M., Michaelson, G., & Shur, Y. (2015). Permafrost soils and carbon cycling. *Soil*, *1*, 147–171.
- Pinheiro, J. C., & Bates, D. M. (2000). *5. Extending the basic linear mixed-effects model*. Mixed Effects Models in S and S-PLUS New York, NY: Springer-Verlag.
- Plaza, C., Pegoraro, E., Bracho, R., Celis, G., Crummer, K. G., Hutchings, J., ... Schuur, E. A. G. Rapid changes in the permafrost soil carbon pool in response to warming. Submitted.
- Poyatos, R., Heinemeyer, A., Ineson, P., Evans, J. G., Ward, H. C., Huntley, B., & Baxter, R. (2014). Environmental and vegetation drivers of seasonal CO₂ fluxes in a sub-arctic forest-mire ecotone. *Ecosystems*, *17*, 377–393.
- R Core Team (2015). *R: A language and environment for statistical computing*. Vienna, Austria: R Foundation for Statistical Computing.
- Romanovsky, V. E., & Osterkamp, T. E. (2000). Effects of unfrozen water on heat and mass transport processes in the active layer and permafrost. *Permafrost and Periglacial Processes*, *11*, 219–239.
- Romanovsky, V. E., Smith, S. L., Christiansen, H. H., Shiklomanov, N. I., Streletskiy, D. A., Drozdov, D. S., ... Marchenko, S. S. (2013). *Permafrost [in Arctic Report Card 2013]*. NOAA. Retrieved from <http://www.arctic.noaa.gov/Report-Card/Report-Card-Archive>
- Salmon, V. G., Soucy, P., Mauritz, M., Celis, G., Natali, S. M., Mack, M. C., & Schuur, E. A. G. (2016). Nitrogen availability increases in a tundra ecosystem during five years of experimental permafrost thaw. *Global Change Biology*, *22*, 1927–1941.
- Schädel, C., Bader, M. K. F., Schuur, E. A. G., Biasi, C., Bracho, R., Capek, P., ... Wickland, K. P. (2016). Potential carbon emissions dominated by carbon dioxide from thawed permafrost soils. *Nature Climate Change*, *6*, 950–953.
- Schuur, E. A. G., Bockheim, J., Canadell, J. G., Euskirchen, E., Field, C. B., Goryachkin, S. V., ... Zimov, S. A. (2008). Vulnerability of permafrost carbon to climate change: Implications for the global carbon cycle. *BioScience*, *58*, 701–714.
- Schuur, E. A. G., Crummer, K. G., Vogel, J. G., & Mack, M. C. (2007). Plant species composition and productivity following permafrost thaw and thermokarst in Alaskan tundra. *Ecosystems*, *10*, 280–292.
- Schuur, E. A. G., McGuire, A. D., Schädel, C., Grosse, G., Harden, J. W., Hayes, D. J., ... Vonk, J. E. (2015). Climate change and the permafrost carbon feedback. *Nature*, *520*, 171–179.
- Schuur, E., Vogel, J., Crummer, K., Lee, H., Sickman, J., & Osterkamp, T. (2009). The effect of permafrost thaw on old carbon release and net carbon exchange from tundra. *Nature*, *459*, 556–559.
- Segal, A. D., & Sullivan, P. F. (2014). Identifying the sources and uncertainties of ecosystem respiration in Arctic tussock tundra. *Biogeochemistry*, *121*, 489–503.
- Serreze, M. C., Walsh, J. E., Chapin, F. S., Osterkamp, T., Dyrugerov, M., Romanovsky, V., ... Barry, R. G. (2000). Observational evidence of recent change in the northern high-latitude environment. *Climatic Change*, *46*, 159–207.
- Shaver, G. R., Johnson, L. C., Cades, D. H., Murray, G., Laundre, J. A., Rastetter, E. R., ... Giblin, A. E. (1998). Biomass and CO₂ flux in wet sedge tundras: Responses to nutrients, temperature, and light. *Ecological Monographs*, *68*, 75–97.
- Shaver, G. R., & Jonasson, S. (1999). Response of Arctic ecosystems to climate change: Results of long-term field experiments in Sweden and Alaska. *Polar Research*, *18*, 245–252.
- Shaver, G. R., Rastetter, E. B., Salmon, V., Street, L. E., van de Weg, M. J., Rocha, A., ... Williams, M. (2013). Pan-Arctic modelling of net ecosystem exchange of CO₂. *Philosophical Transactions of the Royal Society B: Biological Sciences*, *368*, 20120485.
- Sjögersten, S., van der Wal, R., & Woodin, S. J. (2006). Small-scale hydrological variation determines landscape CO₂ fluxes in the high Arctic. *Biogeochemistry*, *80*, 205–216.
- Street, L. E., Shaver, G. R., Williams, M., & Van Wijk, M. T. (2007). What is the relationship between changes in canopy leaf area and changes in photosynthetic CO₂ flux in arctic ecosystems? *Journal of Ecology*, *95*, 139–150.
- Sturm, M., Racine, C., & Tape, K. (2001). Climate change – Increasing shrub abundance in the Arctic. *Nature*, *411*, 546–547.
- Sulman, B. N., Desai, A. R., Schroeder, N. M., Ricciuto, D., Barr, A., Richardson, A. D., & Weng, E. (2012). Impact of hydrological variations on modeling of peatland CO₂ fluxes: Results from the North American Carbon Program site synthesis. *Journal of Geophysical Research: Biogeosciences*, *117*, G01031.
- Tarnocai, C., Canadell, J. G., Mazhitova, G., Schuur, E. A. G., & Kuhry, P. (2009). Soil organic carbon pools in the northern circumpolar permafrost region. *Global Biogeochemical Cycles*, *23*, GB2023.
- Trucco, C., Schuur, E., Natali, S., Belshe, E., Bracho, R., & Vogel, J. (2012). Seven-year trends of CO₂ exchange in a tundra ecosystem affected by long-term permafrost thaw. *Journal of Geophysical Research-Biogeosciences*, *117*, G02031.
- Tuittila, E.-S., Vasander, H., & Laine, J. (2004). Sensitivity of C sequestration in reintroduced sphagnum to water-level variation in a cutaway peatland. *Restoration Ecology*, *12*, 483–493.
- Ueyama, M., Iwata, H., & Harazono, Y. (2014). Autumn warming reduces the CO₂ sink of a black spruce forest in interior Alaska based on a nine-year eddy covariance measurement. *Global Change Biology*, *20*, 1161–1173.
- Ueyama, M., Iwata, H., Harazono, Y., Euskirchen, E. S., Oechel, W. C., & Zona, D. (2013). Growing season and spatial variations of carbon fluxes of Arctic and boreal ecosystems in Alaska (USA). *Ecological Applications*, *23*, 1798–1816.
- Vogel, J., Schuur, E. A. G., Trucco, C., & Lee, H. (2009). Response of CO₂ exchange in a tussock tundra ecosystem to permafrost thaw and thermokarst development. *Journal of Geophysical Research: Biogeosciences*, *114*, G04018.
- Wahren, C. H. A., Walker, M. D., & Bret-Harte, M. S. (2005). Vegetation responses in Alaskan arctic tundra after 8 years of a summer warming and winter snow manipulation experiment. *Global Change Biology*, *11*, 537–552.
- Walker, M. D., Wahren, C. H., Hollister, R. D., Henry, G. H. R., Ahlquist, L. E., Alatalo, J. M., ... Wookey, P. A. (2006). Plant community responses to experimental warming across the tundra biome. *Proceedings of the National Academy of Sciences*, *103*, 1342–1346.
- Walker, M. D., Walker, D. A., Welker, J. M., Arft, A. M., Bardsley, T., Brooks, P. D., ... Turner, P. L. (1999). Long-term experimental manipulation of winter snow regime and summer temperature in arctic and alpine tundra. *Hydrological Processes*, *13*, 2315–2330.
- Webb, E. E., Schuur, E. A. G., Natali, S. M., Oken, K. L., Bracho, R., Krapek, J. P., ... Nickerson, N. R. (2016). Increased wintertime CO₂ loss as a result of sustained tundra warming. *Journal of Geophysical Research: Biogeosciences*, *121*, 249–265.
- Weintraub, M. N., & Schimel, J. P. (2003). Interactions between carbon and nitrogen mineralization and soil organic matter chemistry in arctic tundra soils. *Ecosystems*, *6*, 129–143.
- Weintraub, M. N., & Schimel, J. P. (2005). Nitrogen cycling and the spread of shrubs control changes in the carbon balance of arctic tundra ecosystems. *BioScience*, *55*, 408–415.
- Welker, J. M., Fahnestock, J. T., Henry, G. H. R., O'Dea, K. W., & Chimner, R. A. (2004). CO₂ exchange in three Canadian High Arctic ecosystems: Response to long-term experimental warming. *Global Change Biology*, *10*, 1981–1995.

- van Wijk, M. T., Clemmensen, K. E., Shaver, G. R., Williams, M., Callaghan, T. V., Chapin, F. S., . . . Rueth, H. (2003). Long-term ecosystem level experiments at Toolik Lake, Alaska, and at Abisko, Northern Sweden: Generalizations and differences in ecosystem and plant type responses to global change. *Global Change Biology*, 10, 105–123.
- Zimov, S. A., Schuur, E. A. G., & Chapin, F. S. (2006). Permafrost and the global carbon budget. *Science*, 312, 1612–1613.
- Zona, D., Oechel, W. C., Kochendorfer, J., Paw, U., Salyuk, A. N., Olivas, P. C., . . . Lipson, D. A. (2009). Methane fluxes during the initiation of a large-scale water table manipulation experiment in the Alaskan Arctic tundra. *Global Biogeochemical Cycles*, 23, GB2013.
- Zuur, A. F., Ieno, E. N., Walker, N., Saveliev, A. A., & Smith, G. M. (2009). *Mixed effects models and extensions in ecology with R*. New York, NY: Springer.

SUPPORTING INFORMATION

Additional Supporting Information may be found online in the supporting information tab for this article.

How to cite this article: Mauritz M, Bracho R, Celis G, et al. Nonlinear CO₂ flux response to 7 years of experimentally induced permafrost thaw. *Glob Change Biol*. 2017;00:1–20. <https://doi.org/10.1111/gcb.13661>